

Optimized Training for Multi-Antenna Wireless Energy Transfer in Frequency-Selective Channel

Yong Zeng and Rui Zhang

Abstract

This paper studies the training design problem for multiple-input single-output (MISO) wireless energy transfer (WET) systems in frequency-selective channels, where the frequency-diversity and energy-beamforming gains can be both reaped to maximize the transferred energy by efficiently learning the channel state information (CSI) at the energy transmitter (ET). By exploiting channel reciprocity, a new two-phase channel training scheme is proposed to achieve the diversity and beamforming gains, respectively. In the first phase, pilot signals are sent from the energy receiver (ER) over a selected subset of the available frequency sub-bands, through which the ET determines a certain number of “strongest” sub-bands with largest antenna sum-power gains and sends their ordered indices to the ER. In the second phase, the selected sub-bands are further trained by the ER, so that the ET obtains a refined estimate of the corresponding MISO channels to implement energy beamforming for WET. A training design problem is formulated and optimally solved, which takes into account the channel training overhead by maximizing the *net* harvested energy at the ER, defined as the average harvested energy offset by that consumed in the two-phase training. Moreover, asymptotic analysis is obtained for systems with a large number of antennas or a large number of sub-bands to gain useful insights on the optimal training design. Lastly, numerical results are provided to corroborate our analysis and show the effectiveness of the proposed scheme by optimally balancing the diversity and beamforming gains achieved in MISO WET systems with limited-energy training.

Index Terms

Wireless energy transfer (WET), energy beamforming, channel training, RF energy harvesting, frequency diversity.

I. INTRODUCTION

Wireless energy transfer (WET), by which energy is delivered wirelessly from one location to another without the hassle of connecting cables, has emerged as a promising solution to provide convenient and reliable power supplies for energy-constrained wireless networks, such as radio-frequency identification (RFID) and sensor networks [1], [2]. One enabling technique of WET for long-range applications (say up to tens of meters) is via radio-frequency

The authors are with the Department of Electrical and Computer Engineering, National University of Singapore. (e-mail: {elezeng, elezhang}@nus.edu.sg). R. Zhang is also with the Institute for Infocomm Research, A*SATR, Singapore.

Part of this work has been submitted to the IEEE International Conference on Communications (ICC), London, UK, June 8-12, 2015.

(RF) or microwave propagation, where dedicated energy-bearing signals are sent from the energy transmitter (ET) over a particular frequency band to the energy receiver (ER) for harvesting the received RF energy (see e.g. [2], [3] and the references therein).

The investigation of RF-based WET has a long history (see e.g. [4]), with early works mainly focusing on high-power applications using gigantic antenna apertures and large transmission power to compensate the significant propagation loss over long transmission distance. For instance, in the well-known solar power satellite (SPS) application [5], it is envisioned that antenna apertures on the order of square kilometers are used for delivering giga-watts power collected in space to Earth. During the past decade, the interest in WET has re-emerged, which was mainly driven by the increasing need to provide low-cost and reliable energy supplies to relatively low-power applications, such as RFID and other wireless sensing/monitoring devices, to replace the traditional battery-powered solution that requires frequent manual battery replacement and/or recharging. Besides, since RF signal is able to convey both information and energy, extensive studies have been devoted to unifying both information and energy transfer under the framework so-called simultaneous wireless information and power transfer (SWIPT) [6]–[8]. Various new application scenarios have also been investigated for SWIPT and other wireless-powered communication networks (WPCN) [2], [9], such as cognitive radio networks [10], [11] and relay networks [12]–[15].

The key practical challenge for implementing WET is to improve its energy transfer efficiency, which is mainly limited by the significant power attenuation loss over distance. In line-of-sight (LOS) environment, the efficiency can be enhanced via uni-directional transmission, by designing the antenna radiation patterns to form a single sharp beam towards the ER for energy focusing. Recently, multi-antenna based technique, termed *energy beamforming*, has been proposed for WET [6], where multiple antennas are employed at the ET to more efficiently and flexibly direct wireless energy to one or more ERs via digital beamforming, especially in non-LOS environment with multiple signal paths from the ET to ERs. Similar to the emerging massive multiple-input multiple-output (MIMO) enabled wireless communications (see e.g. [16], [17] and the references therein), by equipping a large number of antennas at the ET, enormous energy beamforming gain can be achieved; hence, the end-to-end energy transfer efficiency can be dramatically enhanced [18].

Besides, for WET in a wide-band regime over frequency-selective channels, the frequency-diversity gain can also be exploited to further improve the energy transfer efficiency, by transmitting more power over the sub-band with higher channel gain. Ideally, maximum energy transfer efficiency is attained by sending just one sinusoid at the frequency that exhibits the strongest channel frequency response [19]. In practice, it may be necessary to spread the transmission power over multiple strong sub-bands in order to comply with various regulations, such as the power spectral density constraint imposed on the license-free ISM (industrial, scientific and medical) band [20]. WET in single- [19], [21], [22] and multi-antenna [23] frequency-selective channels have been studied under the more general SWIPT setup, where perfect channel state information (CSI) is assumed at the transmitter.

In practice, both the energy-beamforming and frequency-diversity gains can be exploited for multi-antenna WET in frequency-selective channels; while they crucially depend on the available CSI at the ET, which needs to be

practically obtained at the cost of additional time and energy consumed. Similar to wireless communication, a direct approach to obtain CSI is by sending pilot signals from the ET to the ER [24], [25], which estimates the corresponding channel and then sends the estimation back to the ET via a finite-rate feedback link (see e.g. [26] and the references therein). However, since the training overhead increases with the number of antennas M at the ET, this method is not suitable when M is large [27]. Furthermore, as pointed out in [28], estimating the channel at the ER requires complex baseband signal processing, which may not be available at the ER due to its practical hardware limitation. A new channel-learning design to cater for the practical RF energy harvesting circuitry at the ER has thus been proposed in [28]. However, the training overhead still increases quickly with M , and can be prohibitive as M becomes large. In [29], by exploiting channel reciprocity between the forward (from the ET to the ER) and reverse (from the ER to the ET) links, we have proposed an alternative channel-learning scheme for WET based on reverse-link training by sending pilot signals from the ER to the ET, which is more efficient since the training overhead is independent of M . Moreover, it is revealed in [29] that a non-trivial trade-off exists in WET systems between maximizing the energy beamforming gain by more accurately estimating the channel at the ET and minimizing the training overhead, including the time and energy used for sending the pilot signals from the ER. To optimally resolve the above trade-off, a training design framework has been proposed in [29] based on maximizing the *net* harvested energy at the ER, which is the average harvested energy offset by that used for channel training. However, the proposed design in [29] applies only for narrowband flat-fading channels instead of the more complex wide-band frequency-selective fading channels, which thus motivates this work.

In this paper, we study the channel learning problem for multiple-input single-output (MISO) point-to-point WET systems over frequency-selective fading channels. Compared to its narrowband counterpart, the channel frequency selectivity in MISO wide-band WET system provides an additional frequency-diversity gain for further enhancement of the energy transfer efficiency. However, the training design also becomes more challenging, since the channels in both the frequency and spatial domains need to be estimated. In particular, achieving the frequency-diversity gain requires only the knowledge of the *total* channel power from all the M transmit antennas at the ET, but for a potentially large number of sub-bands; while the energy beamforming gain relies on a more accurate estimation of the MISO channel (both phase and magnitude for each antenna), but only for a small subset of sub-bands selected with largest channel power for energy transmission. Therefore, an efficient training design for multi-antenna wide-band WET needs to achieve a good balance between exploiting the frequency-diversity gain (by training more independent sub-bands) versus the energy beamforming gain (by allocating more training energy to the selected sub-bands), and yet without consuming excessive energy at the ER, as will be pursued in this paper. Specifically, the main contributions of this paper are summarized as follows:

- First, under channel reciprocity, we propose a new two-phase channel training scheme for MISO wide-band WET, to exploit the frequency-diversity and energy-beamforming gains, respectively. In phase-I training, pilot signals are sent from the ER over a selected subset of the available frequency sub-bands. Based on the received

total energy across all the antennas at the ET over each of the trained sub-bands, the ET determines a certain number of sub-bands with largest antenna sum-power gains and sends their ordered indices to the ER. In phase-II training, the selected sub-bands are further trained by the ER, so that the ET obtains a refined estimate of their MISO channels to implement energy beamforming over them for WET. The proposed training scheme is more efficient than conventional wide-band training for the (exact) MISO channels over all the sub-bands in terms of both energy and spectrum usage.

- Second, based on the order statistic analysis [30], a closed-form expression is derived for the average harvested energy at the ER with the proposed two-phase training scheme, in terms of the number of sub-bands trained, as well as the pilot signal energy allocated in the two training phases. An optimization problem is thus formulated to maximize the *net* harvested energy at the ER, which explicitly takes into account the energy consumption at the ER for sending the pilot signals. The formulated problem is optimally solved based on convex optimization techniques to obtain the optimal training design.
- Third, we provide the asymptotic analysis for systems with a large number of antennas (massive-array WET) or a large number of independent sub-bands (massive-band WET) to gain further insights on the optimal training design. It is shown that while the *net* harvested energy at the ER linearly increases with the number of ET antennas asymptotically, it is upper-bounded by a constant value as the number of independent sub-bands goes to infinity. The latter result is a consequence of the faster increase in training energy cost (linearly) than that in the achieved frequency-diversity gain for WET (logarithmically) as more independent sub-bands are trained.

The rest of this paper is organized as follows. Section II introduces the system model. Section III discusses the proposed two-phase training scheme for MISO wide-band WET and formulates the training optimization problem. In Section IV, the formulated problem is optimally solved to obtain the optimal training strategy. In Section V, asymptotic analysis is provided for massive-array and massive-band WET systems, respectively. Numerical results are provided in Section VI to corroborate our study. Finally, we conclude the paper in Section VII.

Notations: In this paper, scalars are denoted by italic letters. Boldface lower- and upper-case letters denote vectors and matrices, respectively. $\mathbb{C}^{M \times N}$ denotes the space of $M \times N$ complex matrices. $\mathbb{E}[\cdot]$ denotes the expectation operator. \mathbf{I}_M denotes an $M \times M$ identity matrix and $\mathbf{0}$ denotes an all-zero matrix of appropriate dimension. For an arbitrary-size matrix \mathbf{A} , its complex conjugate, transpose, and Hermitian transpose are respectively denoted as \mathbf{A}^* , \mathbf{A}^T and \mathbf{A}^H . $\|\mathbf{x}\|$ denotes the Euclidean norm of vector \mathbf{x} . For a real number x , $[x]^+ \triangleq \max\{x, 0\}$. $a!$ denotes the factorial of a and $\binom{n}{k}$ represents the binomial coefficient. Furthermore, $\mathcal{CN}(\boldsymbol{\mu}, \mathbf{C})$ represents the circularly symmetric complex Gaussian (CSCG) distribution with mean $\boldsymbol{\mu}$ and covariance matrix \mathbf{C} . Finally, for two positive-valued functions $f(x)$ and $g(x)$, the notation $f(x) = \Theta(g(x))$ implies that $\exists c_1, c_2 > 0$ such that $c_1 g(x) \leq f(x) \leq c_2 g(x)$ for sufficiently large x .

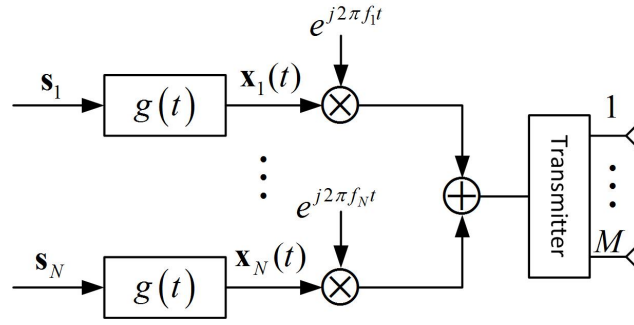


Fig. 1: Schematics of a multi-antenna multi-band wireless energy transmitter.

II. SYSTEM MODEL

We consider a MISO point-to-point WET system in frequency-selective channel, where an ET equipped with $M \geq 1$ antennas is employed to deliver wireless energy to a single-antenna ER. We assume that the total available bandwidth is B , which is equally divided into N orthogonal sub-bands with the n th sub-band centered at frequency f_n and of bandwidth $B_s = B/N$. We assume that $B_s < B_c$, where B_c denotes the channel coherence bandwidth, so that the channel between the ET and ER experiences frequency-flat fading within each sub-band. Denote $\mathbf{h}_n \in \mathbb{C}^{M \times 1}$, $n = 1, \dots, N$, as the complex-conjugated baseband equivalent MISO channel from the ET to the ER in the n th sub-band. We assume a quasi-static Rayleigh fading model, where \mathbf{h}_n remains constant within each block of $T < T_c$ seconds, with T_c denoting the channel coherence time, but can vary from one block to another. Furthermore, the elements in \mathbf{h}_n are modeled as independent and identically distributed (i.i.d.) zero-mean CSCG random variables with variance β , i.e.,

$$\mathbf{h}_n \sim \mathcal{CN}(\mathbf{0}, \beta \mathbf{I}_M), \quad n = 1, \dots, N, \quad (1)$$

where β models the large-scale fading due to shadowing as well as the distance-dependent path loss.

Within each block of T seconds, i.e., $0 \leq t \leq T$, the input-output relation for the forward link energy transmission can be expressed as

$$y_n(t) = \mathbf{h}_n^H \mathbf{x}_n(t) + z_n(t), \quad n = 1, \dots, N, \quad (2)$$

where $y_n(t)$ denotes the received signal at the ER in the n th sub-band; $\mathbf{x}_n(t) \in \mathbb{C}^{M \times 1}$ denotes the baseband energy-bearing signals transmitted by the ET in sub-band n ; and $z_n(t)$ denotes the additive noise at the ER. Different from wireless communication where random signals need to be transmitted to convey information, $\mathbf{x}_n(t)$ in (2) is designated only for energy transmission and thus can be chosen to be deterministic. The average power p_n transmitted over sub-band n can then be expressed as

$$p_n = \frac{1}{T} \int_0^T \|\mathbf{x}_n(t)\|^2 dt, \quad n = 1, \dots, N. \quad (3)$$

At the ER, the incident RF power captured by the antenna is converted to direct current (DC) power for battery replenishment by a device called rectifier [7]. By ignoring the energy harvested from the background noise which

is practically small, the total harvested energy at the ER over all N sub-bands during each block can be expressed as [6]

$$Q = \eta \sum_{n=1}^N \int_0^T |\mathbf{h}_n^H \mathbf{x}_n(t)|^2 dt, \quad (4)$$

where $0 < \eta \leq 1$ denotes the energy conversion efficiency at the ER. Without loss of generality, $\mathbf{x}_n(t)$ can be expressed as (see Fig. 1 for the transmitter schematics)

$$\mathbf{x}_n(t) = \mathbf{s}_n g(t), \quad 0 \leq t \leq T, \quad n = 1, \dots, N, \quad (5)$$

where $\mathbf{s}_n \in \mathbb{C}^{M \times 1}$ denotes the energy beamforming vector for the n th sub-band, and $g(t)$ represents the pulse-shaping waveform (e.g., raised cosine pulse) with normalized power, i.e., $\frac{1}{T} \int_0^T |g(t)|^2 dt = 1$. Note that the bandwidth of $g(t)$, which is approximately equal to $1/T$, needs to be no larger than B_s . We thus have

$$\frac{1}{T_c} < \frac{1}{T} < B_s < B_c,$$

or $T_c B_c > 1$, i.e., a so-called ‘‘under-spread’’ wide-band fading channel is assumed [31].

With (3) and (5), the power p_n transmitted over sub-band n can be expressed as $p_n = \|\mathbf{s}_n\|^2$, $\forall n$. Furthermore, the harvested energy Q in (4) can be written as $Q = \eta T \sum_{n=1}^N |\mathbf{h}_n^H \mathbf{s}_n|^2$. In the ideal case with perfect CSI, i.e., $\{\mathbf{h}_n\}_{n=1}^N$, at the ET, the optimal design of $\{\mathbf{s}_n\}_{n=1}^N$ that maximizes Q can be obtained by solving the following problem

$$\begin{aligned} & \max \eta T \sum_{n=1}^N |\mathbf{h}_n^H \mathbf{s}_n|^2 \\ & \text{subject to } \sum_{n=1}^N \|\mathbf{s}_n\|^2 \leq P_t, \\ & \|\mathbf{s}_n\|^2 \leq P_s, \quad \forall n, \end{aligned} \quad (6)$$

where P_t denotes the maximum transmission power at the ET across all the N sub-bands, and P_s corresponds to the power spectrum density constraint for each sub-band [20]. Without loss of generality, we assume that $P_s \leq P_t \leq NP_s$, since otherwise at least one of the constraint in (6) is redundant and hence can be removed. In addition, for the convenience of exposition, we assume that P_t is a multiple of P_s , i.e., $P_t/P_s = N_2$ for some integer $1 \leq N_2 \leq N$. It can then be obtained that the optimal solution to problem (6) is

$$\mathbf{s}_{[n]} = \begin{cases} \sqrt{P_s} \frac{\mathbf{h}_{[n]}}{\|\mathbf{h}_{[n]}\|}, & n = 1, \dots, N_2, \\ \mathbf{0}, & n = N_2 + 1, \dots, N, \end{cases} \quad (7)$$

where $[\cdot]$ is a permutation such that $\|\mathbf{h}_{[1]}\|^2 \geq \|\mathbf{h}_{[2]}\|^2 \dots \geq \|\mathbf{h}_{[N]}\|^2$. The resulting harvested energy is

$$Q^{\text{ideal}} = \eta T P_s \sum_{n=1}^{N_2} \|\mathbf{h}_{[n]}\|^2. \quad (8)$$

It is observed from (7) that for a MISO multi-band WET system with $P_t < NP_s$, or $N_2 < N$, the optimal scheme is to transmit over the N_2 strongest sub-bands only, each with the maximum allowable power. As a result, the

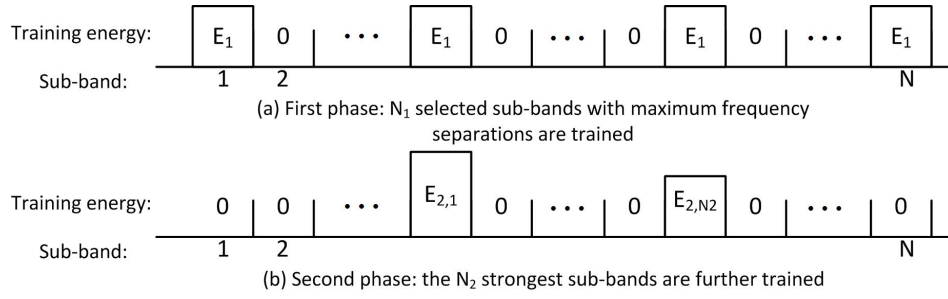


Fig. 2: Two-phase channel training for multi-antenna multi-band wireless energy transfer.

remaining $N - N_2$ unused sub-bands can be opportunistically re-used for other applications such as information transmission. The solution in (7) also shows that for each of the N_2 selected sub-bands, maximum ratio transmission (MRT) should be performed across different transmit antennas to achieve the maximum energy beamforming gain. Moreover, (8) implies that for multi-antenna WET systems in frequency-selective channels, both frequency-diversity and energy beamforming gains should be optimally attained to maximize the energy transfer efficiency in the ideal case with perfect CSI at the ET.

In practice, the CSI needs to be obtained at the ET via channel training and/or feedback from the ER, which are subject to channel estimation and/or feedback errors and incur additional energy and time costs. Consequently, the maximum harvested energy given in (8) cannot be achieved; instead, it only provides a performance upper bound for practical WET systems, for which efficient channel-learning schemes need to be designed. In this paper, by exploiting the channel reciprocity that the forward and reverse link channels are transpose of each other, we propose a two-phase channel training scheme to reap both the frequency-diversity and energy beamforming gains for MISO WET with energy-constrained ER. As illustrated in Fig. 2, the first phase corresponds to the first $\tau_1 < T$ seconds of each block, where pilot signals are sent by the ER to the ET over N_1 out of the N available sub-bands, each with energy E_1 , where $N_2 \leq N_1 \leq N$. By comparing the total received energy from all M antennas at the ET over each of the N_1 trained sub-bands, the ET determines the N_2 strongest sub-bands with largest antenna sum-power gains, and sends their corresponding orders and indices to the ER. In the second phase of $\tau_2 < T - \tau_1$ seconds, additional training signal is sent by the ER over the N_2 selected sub-bands, each with possibly different training energy depending on their relative order as determined in phase I. The ET then obtains an estimate of the MISO channel for each of the N_2 selected sub-bands, based on which MRT beamforming is performed for energy transmission during the remaining $T - \tau_1 - \tau_2$ seconds. The proposed two-phase training scheme is elaborated in more details in the next section.

III. PROBLEM FORMULATION

A. Two-Phase Training

1) *Phase-I Training:* Denote by $\mathcal{N}_1 \subset \{1, \dots, N\}$ the set of the N_1 trained sub-bands in phase I, with $N_2 \leq N_1 \leq N$. To maximize the frequency-diversity gain, the sub-bands with the maximum frequency separations are

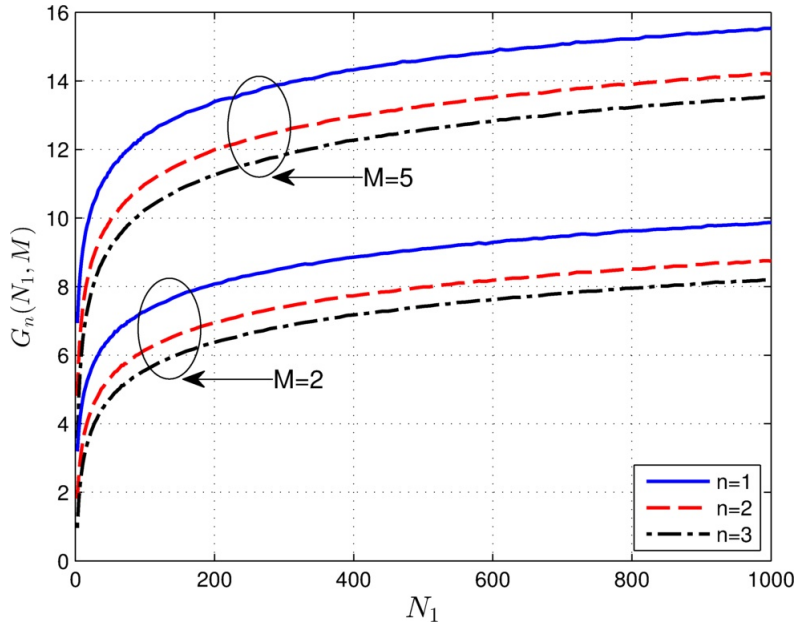


Fig. 3: $G_n(N_1, M)$, $n = 1, 2, 3$, versus N_1 for $M = 2$ and $M = 5$.

selected in \mathcal{N}_1 so that their channels are most likely to be independent (see Fig. 2(a)), e.g., if $N_1 = 2$, we have $\mathcal{N}_1 = \{1, N\}$. The received training signals at the ET can be written as

$$\mathbf{r}_n^I(t) = \sqrt{E_1} \mathbf{h}_n^* \phi_n(t) + \mathbf{w}_n^I(t), \quad 0 \leq t \leq \tau_1, \quad n \in \mathcal{N}_1, \quad (9)$$

where E_1 denotes the training energy used by the ER for each trained sub-band; $\phi_n(t)$ represents the training waveform for sub-band n with normalized energy, i.e., $\int_0^{\tau_1} |\phi_n(t)|^2 dt = 1, \forall n$; and $\mathbf{w}_n^I(t) \in \mathbb{C}^{M \times 1}$ represents the additive white Gaussian noise (AWGN) at the receiver of the ET with power spectrum density N_0 . The total energy consumed at the ER for channel training in this phase is

$$E_{\text{tr}}^I = \sum_{n \in \mathcal{N}_1} \int_0^{\tau_1} |\sqrt{E_1} \phi_n(t)|^2 dt = E_1 N_1. \quad (10)$$

At the ET, the received training signal is first separated over different sub-bands. After complex-conjugate operation, each $\mathbf{r}_n^{I*}(t)$ then passes through a matched filter to obtain

$$\mathbf{y}_n^I = \int_0^{\tau_1} \mathbf{r}_n^{I*}(t) \phi_n(t) dt = \sqrt{E_1} \mathbf{h}_n + \mathbf{z}_n^I, \quad n \in \mathcal{N}_1, \quad (11)$$

where $\mathbf{z}_n^I \sim \mathcal{CN}(\mathbf{0}, N_0 \mathbf{I}_M)$ denotes the i.i.d. AWGN vector. Based on (11), the ET determines the N_2 out of the N_1 trained sub-bands that have the largest power gains. Specifically, the N_1 sub-bands in \mathcal{N}_1 are ordered based on the total received energy across all the M antennas such that

$$\|\mathbf{y}_{[1]}^I\|^2 \geq \|\mathbf{y}_{[2]}^I\|^2 \geq \dots \geq \|\mathbf{y}_{[N_1]}^I\|^2. \quad (12)$$

The ET then sends to the ER the *ordered* indices of the N_2 strongest sub-bands $\mathcal{N}_2 = \{[1], \dots, [N_2]\}$.

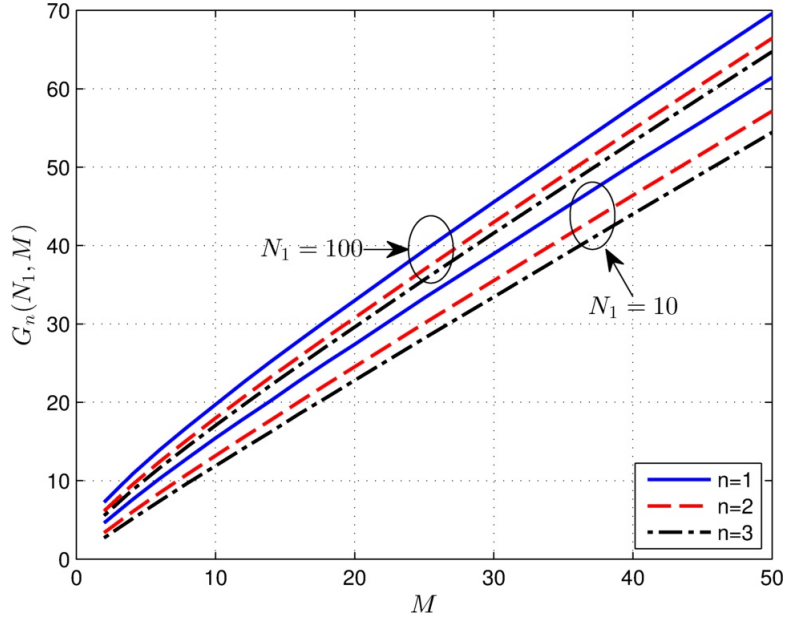


Fig. 4: $G_n(N_1, M)$, $n = 1, 2, 3$, versus M for $N_1 = 10$ and $N_1 = 100$.

2) *Phase-II Training*: In the second phase of τ_2 seconds, additional pilot signals are transmitted by the ER over the N_2 selected sub-bands for the ET to estimate the corresponding MISO channels. Denote by $E_{2,n}$ the training energy used for the n th strongest sub-band as determined in (12), $n = 1, \dots, N_2$. With similar processing as in phase I, the resulting signal at the ET during phase II over sub-band $[n]$ can be expressed as

$$\mathbf{y}_{[n]}^{\text{II}} = \sqrt{E_{2,n}} \mathbf{h}_{[n]} + \mathbf{z}_{[n]}^{\text{II}}, \quad n = 1, \dots, N_2, \quad (13)$$

where $\mathbf{z}_{[n]}^{\text{II}} \sim \mathcal{CN}(\mathbf{0}, N_0 \mathbf{I}_M)$ denotes the AWGN. The ET then performs the linear minimum mean-square error (LMMSE) estimation for $\mathbf{h}_{[n]}$ based on $\mathbf{y}_{[n]}^{\text{II}}$.¹ To obtain the optimal LMMSE estimator, we first provide the following lemma.

Lemma 1: Given that \mathbf{h}_n and \mathbf{h}_m are independent $\forall n, m \in \mathcal{N}_1$ and $n \neq m$, the average power of $\mathbf{h}_{[n]}$, where $[n]$ denotes the n th strongest sub-band determined via phase-I training as in (12), can be expressed as

$$R_n(N_1, E_1) \triangleq \mathbb{E} \left[\|\mathbf{h}_{[n]}\|^2 \right] = \frac{\beta^2 E_1 G_n(N_1, M) + \beta N_0 M}{\beta E_1 + N_0}, \quad n = 1, \dots, N_2, \quad (14)$$

with $G_n(N_1, M)$ an increasing function of N_1 and M as defined in (56) and (57) in Appendix B, which satisfies:

$$G_1(N_1, M) \geq G_2(N_1, M) \geq \dots \geq G_{N_2}(N_1, M) \geq M. \quad (15)$$

Proof: The proof of Lemma 1 requires some basic knowledge of order statistic [30], which is briefly introduced in Appendix A. The detailed proof is given in Appendix C, following a useful lemma presented in Appendix B. ■

¹In principle, $\mathbf{h}_{[n]}$ can be estimated based on both observations $\mathbf{y}_{[n]}^{\text{I}}$ and $\mathbf{y}_{[n]}^{\text{II}}$. To simplify the processing of multi-band energy detection in phase-I training, we assume that $\mathbf{y}_{[n]}^{\text{I}}$ is only used for determining the strongest sub-bands via estimating the power $\|\mathbf{h}_{[n]}\|^2$ while only $\mathbf{y}_{[n]}^{\text{II}}$ is used for estimating the exact MISO channel $\mathbf{h}_{[n]}$.

It can be inferred from Lemma 1 that $R_n(N_1, E_1)$ monotonically increases with the training-energy-to-noise ratio E_1/N_0 . In the extreme case when $E_1/N_0 \rightarrow 0$, for which the energy comparison in (12) is solely determined by the additive noise and hence is unreliable, $R_n(N_1, E_1)$ in (14) reduces to βM , $\forall n$, consistent with the assumed channel statistics in (1). In this case, no frequency-diversity gain is achieved. On the other hand, as $E_1/N_0 \rightarrow \infty$, $R_n(N_1, E_1)$ approaches to its upper bound $\beta G_n(N_1, M)$. Thus, the ratio $G_n(N_1, M)/M$ can be interpreted as the maximum frequency-diversity gain achievable for the n th strongest sub-channel by training N_1 independent sub-bands. As an illustration, Fig. 3 and Fig. 4 plot the numerical values of $G_n(N_1, M)$ for $n = 1, 2, 3$ against N_1 and M , respectively. It is observed that while $G_n(N_1, M)$ increases linearly with M , it scales with N_1 only in a logarithmic manner.

With Lemma 1, the LMMSE estimator of the MISO channels corresponding to the N_2 selected sub-bands in phase-II training can be obtained as follows.

Lemma 2: The LMMSE estimator $\hat{\mathbf{h}}_{[n]}$ for the MISO channel $\mathbf{h}_{[n]}$ based on (13) is

$$\hat{\mathbf{h}}_{[n]} = \frac{\sqrt{E_{2,n} R_n(N_1, E_1)}}{E_{2,n} R_n(N_1, E_1) + N_0 M} \mathbf{y}_{[n]}^{\text{II}}, \quad n = 1, \dots, N_2. \quad (16)$$

Define the channel estimation error as $\tilde{\mathbf{h}}_{[n]} \triangleq \mathbf{h}_{[n]} - \hat{\mathbf{h}}_{[n]}$. We then have

$$\mathbb{E} \left[\|\tilde{\mathbf{h}}_{[n]}\|^2 \right] = \frac{N_0 M R_n(N_1, E_1)}{E_{2,n} R_n(N_1, E_1) + N_0 M}, \quad (17)$$

$$\mathbb{E} \left[\|\hat{\mathbf{h}}_{[n]}\|^2 \right] = \frac{E_{2,n} R_n^2(N_1, E_1)}{E_{2,n} R_n(N_1, E_1) + N_0 M}, \quad (18)$$

$$\mathbb{E} \left[\tilde{\mathbf{h}}_{[n]}^H \hat{\mathbf{h}}_{[n]} \right] = 0, \quad n = 1, \dots, N_2. \quad (19)$$

Proof: Please refer to Appendix D. ■

B. Net Harvested Energy Maximization

After the two-phase training, energy beamforming is performed by the ET over the N_2 selected sub-bands based on the estimated MISO channels $\{\hat{\mathbf{h}}_{[n]}\}_{n=1}^{N_2}$ for WET during the remaining time of $T - \tau_1 - \tau_2$ seconds. According to (7), the energy beamforming vector for the n th selected sub-band is set as $\mathbf{s}_{[n]} = \sqrt{P_s} \hat{\mathbf{h}}_{[n]} / \|\hat{\mathbf{h}}_{[n]}\|$, $n = 1, \dots, N_2$. The resulting energy harvested at the ER can be expressed as²

$$\begin{aligned} \hat{Q} &= \eta T P_s \sum_{n=1}^{N_2} \frac{|\mathbf{h}_{[n]}^H \hat{\mathbf{h}}_{[n]}|^2}{\|\hat{\mathbf{h}}_{[n]}\|^2} \\ &= \eta T P_s \sum_{n=1}^{N_2} \left(\|\hat{\mathbf{h}}_{[n]}\|^2 + \frac{|\tilde{\mathbf{h}}_{[n]}^H \hat{\mathbf{h}}_{[n]}|^2}{\|\hat{\mathbf{h}}_{[n]}\|^2} + \tilde{\mathbf{h}}_{[n]}^H \hat{\mathbf{h}}_{[n]} + \hat{\mathbf{h}}_{[n]}^H \tilde{\mathbf{h}}_{[n]} \right), \end{aligned} \quad (20)$$

²We assume that T is sufficiently large so that $T \gg \tau_1 + \tau_2$; as a result, the time overhead for channel training is ignored (but energy cost of channel training remains).

where we have used the identity $\mathbf{h}_{[n]} = \hat{\mathbf{h}}_{[n]} + \tilde{\mathbf{h}}_{[n]}$ in (20). Based on (17)-(19), the average harvested energy at the ER can be expressed as

$$\begin{aligned} \bar{Q}(N_1, E_1, \{E_{2,n}\}) &= \mathbb{E} \left[\hat{Q} \right] \\ &= \eta T P_s \sum_{n=1}^{N_2} R_n(N_1, E_1) \left(1 - \frac{(M-1)N_0}{E_{2,n}R_n(N_1, E_1) + N_0M} \right). \end{aligned} \quad (21)$$

It is observed from (21) that for each of the N_2 selected sub-bands, the average harvested energy is given by a difference of two terms. The first term, $\eta T P_s R_n(N_1, E_1)$, is the average harvested energy when energy beamforming is based on the perfect knowledge of $\mathbf{h}_{[n]}$ over sub-band $[n]$, where $[n]$ is the n th strongest sub-band determined via phase-I training among the N_1 trained sub-bands each with training energy E_1 . The second term can be interpreted as the loss in energy beamforming performance due to the error in the estimated MISO channel $\hat{\mathbf{h}}_{[n]}$ in phase-II training. For the extreme scenario with $E_{2,n}/N_0 \rightarrow \infty$ so that $\mathbf{h}_{[n]}$ is perfectly estimated, or in SISO system ($M = 1$) for which no energy beamforming can be applied, the second term in (21) vanishes, as expected.

The *net* harvested energy at the ER, which is the average harvested energy offset by that used for sending pilot signals in the two-phase training, can be expressed as

$$\bar{Q}_{\text{net}}(N_1, E_1, \{E_{2,n}\}) = \bar{Q}(N_1, E_1, \{E_{2,n}\}) - E_1 N_1 - \sum_{n=1}^{N_2} E_{2,n}. \quad (22)$$

The problem of finding the optimal training design to maximize \bar{Q}_{net} can be formulated as

$$\begin{aligned} \text{(P1):} \quad & \max_{N_1, E_1, \{E_{2,n}\}} \bar{Q}_{\text{net}}(N_1, E_1, \{E_{2,n}\}) \\ & \text{subject to} \quad N_2 \leq N_1 \leq N, \\ & \quad \quad \quad E_1 \geq 0, \quad E_{2,n} \geq 0, \quad n = 1, \dots, N_2. \end{aligned}$$

In the following sections, we first develop an efficient algorithm to obtain the optimal solution to (P1), and then investigate the problem in the asymptotic regime with large M or large N to gain useful insights.

IV. OPTIMAL TRAINING DESIGN

To find the optimal solution to (P1), we first obtain the optimal training energy $\{E_{2,n}\}_{n=1}^{N_2}$ in phase II with N_1 and E_1 fixed. In this case, (P1) can be decoupled into N_2 parallel sub-problems. By discarding constant terms, the n th sub-problem can be formulated as

$$\min_{E_{2,n} \geq 0} \frac{(M-1)N_0 \eta T P_s R_n(N_1, E_1)}{E_{2,n} R_n(N_1, E_1) + N_0 M} + E_{2,n}. \quad (23)$$

Problem (23) is convex, whose optimal solution can be expressed in closed-form as

$$E_{2,n}^*(N_1, E_1) = \left[\sqrt{\eta T P_s (M-1) N_0} - \frac{N_0 M}{R_n(N_1, E_1)} \right]^+, \quad n = 1, \dots, N_2. \quad (24)$$

The solution in (24) implies that non-zero training energy should be allocated for the n th strongest sub-band in phase II only if its expected channel power $R_n(N_1, E_1)$ is sufficiently large. Furthermore, (24) has a nice water-filling

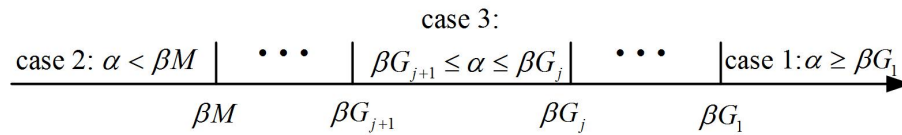


Fig. 5: Three different cases for solving problem (28).

interpretation, with fixed water level $\sqrt{\eta T P_s (M-1) N_0}$ and different base levels that depend on the expected channel power gain $R_n(N_1, E_1)$. For sub-bands with larger $R_n(N_1, E_1)$, more training energy should be allocated to achieve better MISO channel estimation, as expected.

The corresponding optimal value of (23) can be expressed as

$$v_n^*(N_1, E_1) = \begin{cases} \frac{M-1}{M} \eta T P_s R_n(N_1, E_1) & \text{if } R_n(N_1, E_1) \leq \alpha, \\ 2\sqrt{(M-1)N_0\eta T P_s} - \frac{N_0 M}{R_n(N_1, E_1)}, & \text{otherwise,} \end{cases} \quad (25)$$

where $\alpha \triangleq \sqrt{N_0 M} / \sqrt{\eta T P_s (M-1)}$. By substituting (25) into (22), the objective function of (P1) in terms of N_1 and E_1 only can be expressed as

$$\bar{Q}_{\text{net}}(N_1, E_1) = \sum_{n=1}^{N_2} \left[\eta T P_s R_n(N_1, E_1) - v_n^*(N_1, E_1) \right] - N_1 E_1. \quad (26)$$

As a result, (P1) reduces to

$$\begin{aligned} & \max_{E_1, N_1} \bar{Q}_{\text{net}}(N_1, E_1) \\ & \text{subject to } N_2 \leq N_1 \leq N, E_1 \geq 0. \end{aligned} \quad (27)$$

To find the optimal solution to problem (27), we first obtain the optimal training energy E_1 with N_1 fixed by solving the following problem,

$$\max_{E_1 \geq 0} \bar{Q}_{\text{net}}(N_1, E_1). \quad (28)$$

Denote by $E_1^*(N_1)$ and $\bar{Q}_{\text{net}}^*(N_1)$ the optimal solution and optimal value of problem (28), respectively. The original problem (P1) then reduces to determining the optimal number of training sub-bands N_1 as

$$N_1^* = \arg \max_{N_2 \leq N_1 \leq N} \bar{Q}_{\text{net}}^*(N_1), \quad (29)$$

which can be easily solved by one-dimensional search. Therefore, the remaining task for solving (P1) is to find the optimal solution to problem (28). To achieve this end, it is first noted from (14) that for any fixed N_1 , as the training energy E_1 varies from 0 to ∞ , $R_n(N_1, E_1)$ monotonically increases from βM to $\beta G_n(N_1, M)$, i.e.,

$$\beta M \leq R_n(N_1, E_1) \leq \beta G_n(N_1, M), \quad \forall E_1 \geq 0, n = 1, \dots, N_2. \quad (30)$$

With this observation, together with the property of $G_n(N_1, M)$ given in (15), problem (28) can be solved by separately considering the following three cases, as illustrated in Fig. 5.

Case 1: $\alpha \geq \beta G_1(N_1, M)$, or $(M-1)\Gamma \leq \frac{M^2}{G_1^2(N_1, M)}$, where

$$\Gamma \triangleq \frac{\eta T P_s \beta^2}{N_0} \quad (31)$$

is referred to as the two-way effective signal-to-noise ratio (ESNR). Note that the term β^2 in Γ captures the effect of two-way signal attenuation due to both the reverse-link training and forward-link energy transmission. In this case, we have $R_n(N_1, E_1) \leq \alpha$ and $E_{2,n}^*(N_1, E_1) = 0$, $\forall n = 1, \dots, N_2$ and $E_1 \geq 0$. In other words, phase-II training should not be performed due to the limited energy beamforming gains. Therefore, $\bar{Q}_{\text{net}}(N_1, E_1)$ in (26) reduces to

$$\bar{Q}_{\text{net}}(N_1, E_1) = \eta TP_s \sum_{n=1}^{N_2} \frac{R_n(N_1, E_1)}{M} - E_1 N_1, \quad \forall E_1 \geq 0. \quad (32)$$

By substituting $R_n(N_1, E_1)$ with (14), problem (28) reduces to

$$\max_{E_1 \geq 0} \eta TP_s \beta \sum_{n=1}^{N_2} \frac{\beta E_1 G_n(N_1, M)/M + N_0}{\beta E_1 + N_0} - E_1 N_1, \quad (33)$$

which is a convex optimization problem with the optimal solution given by

$$E_1^*(N_1) = \sqrt{\eta TP_s N_0} \left[\sqrt{\frac{\sum_{n=1}^{N_2} \left(\frac{G_n(N_1, M)}{M} - 1 \right)}{N_1}} - \frac{1}{\sqrt{\Gamma}} \right]^+. \quad (34)$$

The corresponding optimal value of (33) can be expressed as

$$\bar{Q}_{\text{net}}^*(N_1) = \begin{cases} \eta TP_s \beta N_2, & \text{if } \sum_{n=1}^{N_2} \left(\frac{G_n(N_1, M)}{M} - 1 \right) < \frac{N_1}{\Gamma} \\ \eta TP_s \beta \left(N_2 + \left(\sqrt{\sum_{n=1}^{N_2} \left(\frac{G_n(N_1, M)}{M} - 1 \right)} - \sqrt{\frac{N_1}{\Gamma}} \right)^2 \right), & \text{otherwise.} \end{cases} \quad (35)$$

It is observed from (34) that for any fixed N_1 , non-zero training energy should be allocated in phase I only if the frequency-diversity gain normalized by N_1 is sufficiently large. In this case, the *net* harvested energy is given by a summation of that achieved in the case without CSI at the ET, $\eta TP_s \beta N_2$, and an additional gain due to the exploitation of frequency diversity, as shown in (35).

Case 2: $\alpha < \beta M$, or $(M-1)\Gamma > 1$. In this case, it follows from (30) that $R_n(N_1, E_1) > \alpha$ and $E_{2,n}^*(N_1, E_1) > 0$, $\forall n = 1, \dots, N_2$ and $E_1 \geq 0$. In other words, regardless of the training energy E_1 in phase I, non-zero training energy should be allocated to each of the N_2 selected sub-bands in phase II due to the potentially large beamforming gains. As a result, it follows from (25) that $\bar{Q}_{\text{net}}(N_1, E_1)$ in (26) can be expressed as

$$\bar{Q}_{\text{net}}(N_1, E_1) = \sum_{n=1}^{N_2} \left[\eta TP_s R_n(N_1, E_1) - 2\sqrt{(M-1)N_0\eta TP_s} + \frac{N_0 M}{R_n(N_1, E_1)} \right] - N_1 E_1. \quad (36)$$

By substituting $R_n(N_1, E_1)$ with (14) and after discarding constant terms, problem (28) can be reformulated as

$$\max_{E_1 \geq 0} \eta TP_s \beta \sum_{n=1}^{N_2} \frac{\beta E_1 G_n(N_1, M) + N_0 M}{\beta E_1 + N_0} + \frac{N_0 M}{\beta} \sum_{n=1}^{N_2} \frac{\beta E_1 + N_0}{\beta E_1 G_n(N_1, M) + N_0 M} - E_1 N_1. \quad (37)$$

Problem (37) belongs to the class of optimizing the sum of linear fractional functions, which is difficult to be optimally solved in general. However, with some manipulations, problem (37) can be simplified into

$$\min_{E_1 \geq 0} f(E_1) \triangleq \frac{b_0}{E_1 + c_0} + E_1 N_1 - \sum_{n=1}^{N_2} \frac{b_n}{E_1 + c_n}, \quad (38)$$

where

$$\begin{aligned} b_0 &= \eta TP_s N_0 \sum_{n=1}^{N_2} (G_n(N_1, M) - M), \quad c_0 = \frac{N_0}{\beta}, \\ b_n &= \frac{N_0^2 M \left(1 - \frac{M}{G_n(N_1, M)}\right)}{\beta^2 G_n(N_1, M)}, \quad c_n = \frac{N_0 M}{\beta G_n(N_1, M)}, \quad n = 1, \dots, N_2. \end{aligned} \quad (39)$$

Problem (38) is still non-convex due to the non-convex objective function. However, by examining its Karush-Kuhn-Tucker (KKT) necessary conditions for global optimality (not necessarily sufficient due to non-convexity in general), the optimal solution to problem (38) must belong to the set

$$\mathcal{E}_1 \triangleq \{0\} \cup \left\{ E_1 > 0 \mid \frac{\partial f(E_1)}{\partial E_1} = 0 \right\}.$$

It can be shown that finding the stationary points satisfying $\frac{\partial f(E_1)}{\partial E_1} = 0$ is equivalent to determining the roots of the following polynomial equation,

$$N_1(E_1 + c_0)^2 \prod_{i=1}^{N_2} (E_1 + c_i)^2 + (E_1 + c_0)^2 \sum_{n=1}^{N_2} b_n \prod_{i=1, i \neq n}^{N_2} (E_1 + c_i)^2 - b_0 \prod_{i=1}^{N_2} (E_1 + c_i)^2 = 0,$$

which has order $2N_2 + 2$ and hence can be efficiently solved numerically for moderate N_2 values. The cardinality of \mathcal{E}_1 is thus bounded by $|\mathcal{E}_1| \leq 2N_2 + 3$. Therefore, the optimal solution to problem (38) can be readily obtained by comparing at most $2N_2 + 3$ candidate solutions as

$$E_1^*(N_1) = \arg \min_{E_1 \in \mathcal{E}_1} f(E_1). \quad (40)$$

With $E_1^*(N_1)$ determined, the corresponding optimal value of problem (28) for the case $\alpha < \beta M$ can be obtained by direct substitution based on (36).

Case 3: $\beta G_{j+1}(N_1, M) \leq \alpha \leq \beta G_j(N_1, M)$, or $\frac{M^2}{G_j^2(N_1, M)} \leq (M-1)\Gamma \leq \frac{M^2}{G_{j+1}^2(N_1, M)}$, for some $j = 1, \dots, N_2$. For convenience, we define $G_{N_2+1}(N_1, M) \triangleq \beta M$. Based on (15) and (30), we have $R_n(N_1, E_1) \leq \alpha$, $\forall n = j+1, \dots, N_2$ and $E_1 \geq 0$. On the other hand, for $n = 1, \dots, j$, $R_n(N_1, E_1)$ may be larger or smaller than α , depending on the training energy E_1 . Let E_1 be chosen such that $R_{k+1}(N_1, E_1) \leq \alpha \leq R_k(N_1, E_1)$ for some $k = 0, \dots, j$. Then based on (14), we must have $E_1 \in [E_1^{(k)}, E_1^{(k+1)}]$, where $E_1^{(k)} \triangleq \frac{N_0(\alpha - \beta M)}{\beta(\beta G_k(N_1, M) - \alpha)}$. For convenience, we define $E_1^{(j+1)} = \infty$ and $E_1^{(0)} = 0$. For E_1 belonging to the above interval, we have $R_n(N_1, E_1) \geq \alpha$, $\forall n = 1, \dots, k$, and $R_n(N_1, E_1) \leq \alpha$, $\forall n = k+1, \dots, j$. Therefore, depending on the $j+1$ intervals in which E_1 lies, $\bar{Q}_{\text{net}}(N_1, E_1)$ in (26) can be explicitly written as

$$\bar{Q}_{\text{net}}(N_1, E_1) = f_k(E_1), \quad \text{for } E_1 \in [E_1^{(k)}, E_1^{(k+1)}], \quad k = 0, \dots, j, \quad (41)$$

where

$$\begin{aligned} f_k(E_1) &\triangleq \sum_{n=1}^k \left(\eta TP_s R_n(N_1, E_1) - 2\sqrt{(M-1)N_0\eta TP_s} + \frac{N_0 M}{R_n(N_1, E_1)} \right) \\ &+ \sum_{n=k+1}^{N_2} \left(\eta TP_s R_n(N_1, E_1) - \frac{M-1}{M} \eta TP_s R_n(N_1, E_1) \right) - N_1 E_1. \end{aligned} \quad (42)$$

As a result, problem (28) for Case 3 can be decomposed into $j + 1$ parallel sub-problems by optimizing E_1 over each of the $j + 1$ intervals, with the k th sub-problem formulated as

$$\begin{aligned} & \max_{E_1} f_k(E_1) \\ & \text{subject to } E_1^{(k)} \leq E_1 \leq E_1^{(k+1)}. \end{aligned} \quad (43)$$

Denote by $E_{1,k}^*$ the optimal solution to the k th sub-problem (43). The solution E_1^* to problem (28) is thus given by

$$E_1^*(N_1) = \arg \max_{E_{1,k}^*, k=0, \dots, j} f_k(E_{1,k}^*), \quad (44)$$

which can be readily determined. Thus, the remaining task is to solve problem (43). With some simple manipulations and after discarding irrelevant terms, problem (43) can be reformulated as

$$\min_{E_1^{(k)} \leq E_1 \leq E_1^{(k+1)}} \frac{d_0}{E_1 + c_0} + E_1 N_1 - \sum_{n=1}^k \frac{b_n}{E_1 + c_n}, \quad (45)$$

where c_0 , b_n , and c_n , for $n = 1, \dots, k$, are defined in (39), and

$$d_0 \triangleq \eta T P_s N_0 \left(\sum_{n=1}^k (G_n(N_1, M) - M) + \sum_{n=k+1}^{N_2} \left(\frac{G_n(N_1, M)}{M} - 1 \right) \right).$$

Note that problem (45) has identical structure as problem (38) and thus can be optimally solved with the same technique as discussed above.

The algorithm for optimally solving the training optimization problem (P1) is summarized as follows.

Algorithm 1 Optimal Solution to (P1)

- 1: **for** $N_1 = N_2, \dots, N$ **do**
 - 2: **if** $\alpha \geq \beta G_1(N_1, M)$ **then**
 - 3: Obtain $E_1^*(N_1)$ and $\bar{Q}_{\text{net}}^*(N_1)$ based on (34) and (35), respectively.
 - 4: **else if** $\alpha < \beta M$ **then**
 - 5: Obtain $E_1^*(N_1)$ and the corresponding $\bar{Q}_{\text{net}}^*(N_1)$ based on (40) and (36), respectively.
 - 6: **else**
 - 7: Determine $j \in \{1, \dots, N_2\}$ such that $\beta G_{j+1}(N_1, M) \leq \alpha \leq \beta G_j(N_1, M)$
 - 8: **for** $k = 0, \dots, j$ **do**
 - 9: Find $E_{1,k}^*$ by solving (45) and obtain the corresponding $f_k(E_{1,k}^*)$ based on (42).
 - 10: **end for**
 - 11: Obtain $E_1^*(N_1)$ and the corresponding $\bar{Q}_{\text{net}}^*(N_1)$ based on (44) and (41), respectively.
 - 12: **end if**
 - 13: **end for**
 - 14: Obtain N_1^* and the corresponding E_1^* based on (29).
 - 15: Obtain $E_{2,n}^*$, $n = 1, \dots, N_2$, based on (24) with N_1^* and E_1^* .
-

V. ASYMPTOTIC ANALYSIS

In this section, we provide an asymptotic analysis for the training optimization problem (P1) with either a large number of ET antennas M (massive-array WET) or a large number of sub-bands N (massive-band WET), from which we draw important insights.

A. Massive-Array WET

Massive MIMO has emerged as one of the key enabling technologies for 5G wireless communication systems due to its tremendous improvement on energy and spectrum efficiency by deploying a very large number of antennas (say, hundreds or even more) at the base stations [16], [17]. For WET systems with a large number of antennas deployed at the ET, it is expected that the energy transfer efficiency can be similarly enhanced, provided that the channel is properly learned at the ET to achieve the enormous beamforming gain. To obtain the asymptotic analysis for (P1) with $M \gg 1$, we first present the following lemma.

Lemma 3: For the function $G_n(N_1, M)$ defined in Lemma 9 in Appendix B, the following asymptotic result holds:

$$G_n(N_1, M) \rightarrow M, \quad \forall n, N_1, \text{ as } M \rightarrow \infty. \quad (46)$$

Proof: For the N_1 i.i.d. CSCG random vectors $\mathbf{v}_i \sim \mathcal{CN}(\mathbf{0}, \sigma_v^2 \mathbf{I}_M)$ given in Lemma 9, the following asymptotic result holds as $M \rightarrow \infty$ due to the law of large numbers:

$$\frac{1}{M} \|\mathbf{v}_i\|^2 \rightarrow \sigma_v^2, \quad \forall i = 1, \dots, N_1.$$

Therefore, we have $\mathbb{E}[\|\mathbf{v}_{[n]}\|^2] \rightarrow \sigma_v^2 M, \forall n$, which thus leads to (46) by definition. \blacksquare

Lemma 4: For MISO WET systems in frequency-selective channels with M transmit antennas and N independent sub-bands, as $M \rightarrow \infty$, the optimized two-phase training scheme reduces to

$$E_1^{\text{large-}M} \rightarrow 0, \quad (47)$$

$$E_{2,n}^{\text{large-}M} \rightarrow \sqrt{\eta T P_s N_0 M}, \quad n = 1, \dots, N_2. \quad (48)$$

Furthermore, the resulting net harvested energy scales linearly with M as

$$\bar{Q}_{\text{net}}^{\text{large-}M} \rightarrow \eta T N_2 P_s \beta M. \quad (49)$$

Proof: Please refer to Appendix E. \blacksquare

Lemma 4 shows that due to the so-called ‘‘channel hardening’’ effect for large M , i.e., $\|\mathbf{h}_n\|^2 \rightarrow \beta M, \forall n = 1, \dots, N$, as $M \rightarrow \infty$, all the N sub-bands have essentially identical power gain βM . Therefore, the frequency-diversity gain vanishes and hence phase-I training is no longer required (see (47)). Moreover, it is observed from (48) that as M increases, the training energy in phase II for each of the selected sub-band scales with M in a square root manner. Since the beamforming gain increases linearly with M , which dominates the training energy cost at large M , the *net* harvested energy scales linearly with M , as shown in (49).

Lemma 5: For MISO WET systems in frequency-selective channels with M transmit antennas and N independent sub-bands, as $M \rightarrow \infty$, the average harvested energy in the ideal case with perfect CSI at the ET scales with M as

$$\bar{Q}^{\text{ideal}} \rightarrow \eta T N_2 P_s \beta M. \quad (50)$$

Proof: With perfect CSI at the ET, the maximum harvested energy for each channel realization has been obtained in (8). The average value taken over all channel realizations can then be obtained as

$$\begin{aligned} \bar{Q}^{\text{ideal}} &= \mathbb{E} [Q^{\text{ideal}}] = \eta T P_s \sum_{n=1}^{N_2} \mathbb{E} [\|\mathbf{h}_{[n]}\|^2] \\ &= \eta T P_s \sum_{n=1}^{N_2} \beta G_n(N, M) \end{aligned} \quad (51)$$

$$\rightarrow \eta T N_2 P_s \beta M, \quad (52)$$

where (51) follows from the definition of the function $G_n(N_1, M)$ given in Lemma 9 in Appendix B, and (52) is true due to Lemma 3. ■

It immediately follows from Lemma 4 and Lemma 5 that for MISO WET systems in frequency-selective channels with M transmit antennas and N independent sub-bands, the proposed two-phase training scheme achieves the optimal asymptotic scaling with M .

B. Massive-Band WET

In this subsection, we investigate the WET system with an asymptotically large bandwidth B , or equivalently, with an unlimited number of sub-bands N . We first study the asymptotic scaling of the average harvested energy at the ER with N under the ideal case with perfect CSI at the ET.

Lemma 6: For MISO WET systems in frequency-selective channels with M transmit antennas and N independent sub-bands, as $N \rightarrow \infty$, the average harvested energy $\bar{Q}^{\text{ideal}}(N)$ in the ideal case with perfect CSI at the ET scales logarithmally with N , i.e., $\bar{Q}^{\text{ideal}}(N) = \Theta(\ln N)$.

Proof: Please refer to Appendix F. ■

Lemma 7: For MISO WET systems in frequency-selective channels with M transmit antennas and N independent sub-bands, as $N \rightarrow \infty$, the net harvested energy $\bar{Q}^{\text{large-}N}$ with the proposed two-phase training scheme is upper-bounded by

$$\bar{Q}^{\text{large-}N} \leq \eta T N_2 P_2 \beta M \left(1 + \left(\sqrt{W(\Gamma N_2 M)} - \frac{1}{\sqrt{W(\Gamma N_2 M)}} \right)^2 \right), \quad (53)$$

where Γ is the two-way ESNR defined in (31), and $W(z)$ is the Lambert W function defined by $z = W(z)e^{W(z)}$.

Proof: Please refer to Appendix G. ■

Lemma 7 shows that, different from the asymptotic linear scaling with the number of transmit antennas M as in Lemma 4, the *net* harvested energy at the ER does not asymptotically increase with N as N becomes large; instead, it

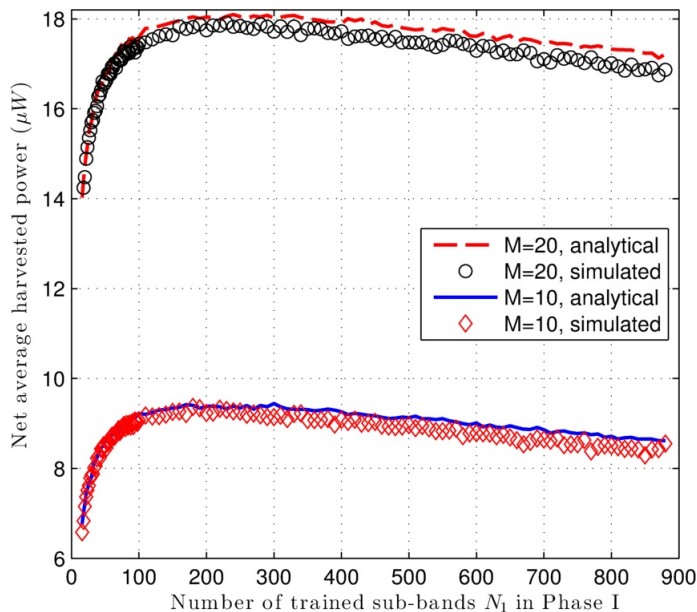


Fig. 6: Net average harvested power versus the number of trained sub-bands N_1 for $M = 10$ and $M = 20$.

is upper-bounded by a constant value that depends on the two-way ESNR, Γ . This result is unsurprising, since while the energy cost ($E_1 N_1$) for channel training in phase I increases linearly with the number of trained sub-bands, the frequency-diversity gain scales only in a logarithmic manner with N_1 , as shown in Lemma 6. Consequently, beyond some large value of N , the benefit of channel training for exploiting the frequency-diversity gain cannot compensate the training energy cost; thus, further bandwidth expansion does not provide any performance improvement in terms of the *net* harvested energy at the ER.

VI. NUMERICAL RESULTS

In this section, numerical examples are provided to corroborate our study. To model the frequency-selective channel, we assume a multi-path power delay profile with exponential distribution $A(\tau) = \frac{1}{\sigma_{\text{rms}}} e^{-\tau/\sigma_{\text{rms}}}$, $\tau \geq 0$, where σ_{rms} denotes the root-mean-square (rms) delay spread. We set $\sigma_{\text{rms}} = 1\mu\text{s}$ so that the 50% channel coherence bandwidth [32], i.e., the frequency separation for which the amplitude correlation is 0.5, is $B_c = \frac{1}{2\pi\sigma_{\text{rms}}} \approx 160$ kHz. We assume that the system is operated over the 902-928MHz ISM band, which is equally divided into $N = 866$ sub-bands each with bandwidth $B_s = 30\text{kHz}$. To comply with the FCC (Federal Communications Commission) regulations over this band [20], (Part 15.247, paragraph (e): the power spectral density from the intentional radiator “shall not be greater than 8dBm in any 3kHz band”), we set the transmission power for each sub-band as $P_s = 60\text{mW}$. Furthermore, according to the FCC regulations Part 15.247, paragraph (b) (3), the maximum output power over the 902-928MHz band shall not exceed 1watt, i.e., $P_t \leq 1\text{watt}$. Therefore, at each instance, the maximum number of sub-bands that can be activated for energy transmission is $N_2 = \lfloor P_t/P_s \rfloor = 16$. We assume that the power spectrum density of the training noise received at the ET is $N_0 = -160\text{dBm/Hz}$. The average power attenuation between the ET and the ER is assumed to be 60dB, i.e., $\beta = 10^{-6}$, which corresponds

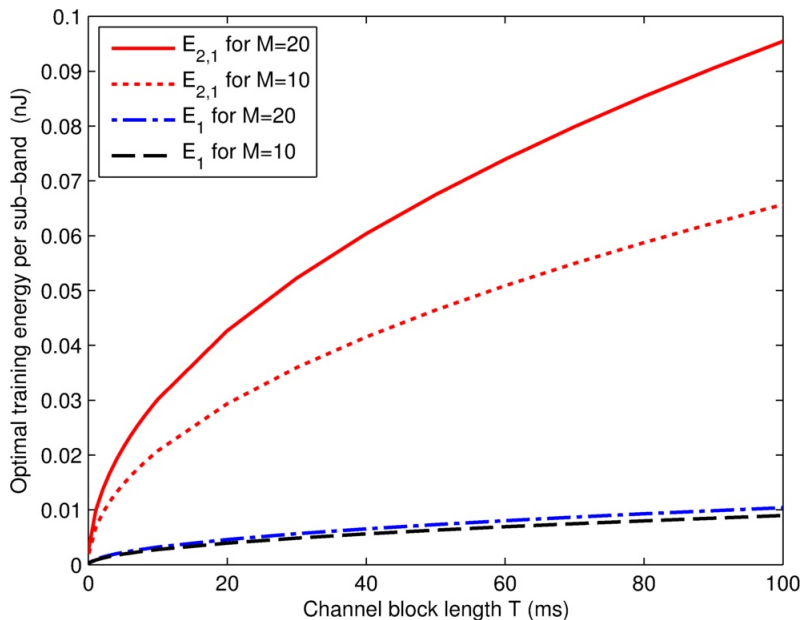


Fig. 7: Optimal training energy E_1 and $E_{2,1}$ versus block length T for $M = 10$ and $M = 20$.

to an operating distance about 30 meters for carrier frequency around 900MHz. Furthermore, we assume that the energy conversion efficiency at the ER is $\eta = 0.8$.

In Fig. 6, by varying the number of sub-bands N_1 that are trained in phase I, the net average harvested power achieved by the optimized two-phase training scheme is plotted for $M = 10$ and $M = 20$, where the average is taken over 10^4 random channel realizations. The channel block length is set as $T = 0.05$ ms. The analytical result obtained in Section IV, i.e., $\bar{Q}_{\text{net}}^*(N_1)/T$ with $\bar{Q}_{\text{net}}^*(N_1)$ denoting the optimal value of problem (28), is also shown in Fig. 6. It is observed that the simulation and analytical results match quite well with each other, which thus validates our theoretical studies. Furthermore, Fig. 6 shows that there is an optimal number of sub-bands to be trained for maximizing the net harvested energy, due to the non-trivial trade-off between achieving more frequency-diversity gain (with larger N_1) and reducing the training energy ($E_1 N_1$ in phase I).

In Fig. 7, the optimal training energy per sub-band E_1 in phase I and that for the strongest sub-band $E_{2,1}$ in phase II are plotted against the channel block length T , with T ranging from 0.1 to 100ms. It is observed that E_1 and $E_{2,1}$ both increase with T , which is expected since as the block length increases, more training energy is affordable due to the increased energy harvested during each block. It is also observed from Fig. 7 that more training energy should be allocated for system with $M = 20$ than that with $M = 10$, since energy beamforming is more effective and hence training is more beneficial when more antennas are available at the ET. Furthermore, for both cases of $M = 10$ and $M = 20$, $E_{2,1}$ is significantly larger than E_1 , since in phase II, only the N_2 selected sub-bands need to be further trained, whereas the training energy in phase I needs to be distributed over $N_1 \gg N_2$ sub-bands to exploit the frequency-diversity.

In Fig. 8, the net average harvested power based on the proposed two-phase training scheme is plotted against block length T , with T ranging from 0.1 to 10ms. The number of antennas at the ET is $M = 20$. The following

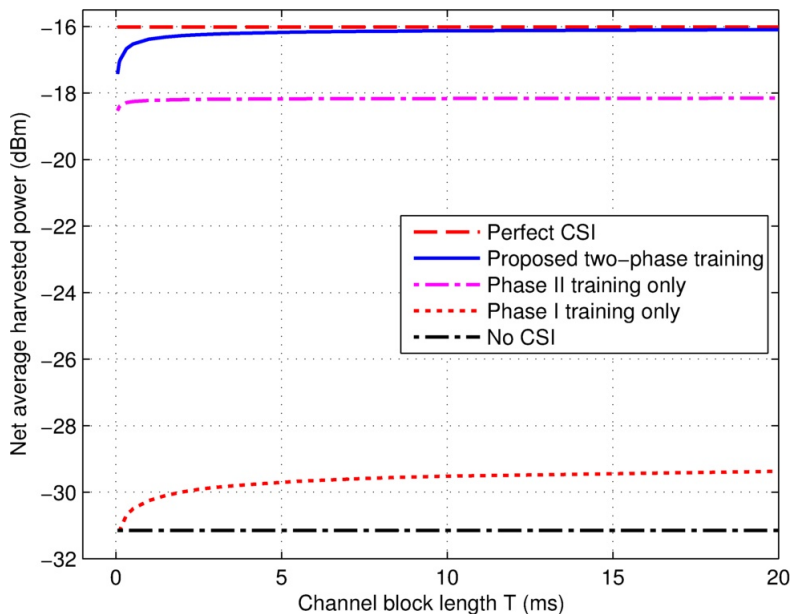


Fig. 8: Net average harvested power versus block length T for $M = 20$.

four benchmark schemes are also considered for comparison.

- 1) *Perfect CSI*: In this case, ideal energy beamforming as given in (7) can be performed and the average harvested energy is given in (51). This corresponds to the performance upper bound since the frequency-diversity and energy-beamforming gains are maximally attained without any energy cost for CSI acquisition.
- 2) *No CSI*: In this case, N_2 out of the N total available sub-bands are randomly selected and isotropic energy transmission is performed over each of the selected sub-band. The resulting average harvested energy at the ER can be expressed as $\bar{Q}_{\text{noCSI}} = \eta T P_s \beta N_2$. Neither frequency-diversity nor beamforming gain is achieved in this case.
- 3) *Phase-I training only*: This corresponds to the special case of the proposed two-phase training scheme with $E_{2,n} = 0, \forall n$. Thus, only frequency-diversity gain is exploited.
- 4) *Phase-II training only*: This corresponds to the special case of the two-phase training scheme with $E_1 = 0$. Thus, only energy beamforming gain is exploited.

It is observed from Fig. 8 that the proposed two-phase training scheme approaches to the performance upper bound with perfect CSI as T increases, and significantly outperforms the other three benchmark schemes. It can also be inferred from the figure that for multi-antenna WET systems in frequency-selective channels, exploiting either frequency-diversity gain (with phase-I training only) or energy beamforming gain (with phase-II training only) is far from optimal in general; instead, a good balance between these two gains as achieved in the proposed two-phase training optimization is needed.

In Fig. 9, to investigate the massive-array case with large M , the net average harvested power is plotted against the number of antennas M at the ET for $T = 1\text{ms}$. It is observed that both the schemes of no-CSI and phase-I training only result in poor performance. On the other hand, for the two training schemes that exploit energy beamforming

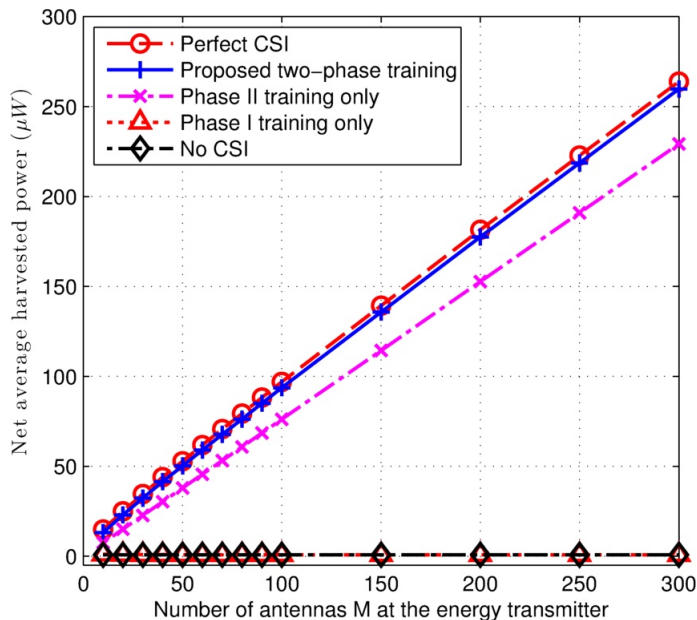


Fig. 9: Net average harvested power versus number of antennas M at the ET.

gain (two-phase training and phase-II training only), the *net* average harvested power scales linearly with M , which is in accordance to Lemma 4. It is also observed from Fig. 9 that, under this setup, the optimized two-phase training still provides considerable performance gain over the phase-II training only, although the performance gap becomes inconsequential for extremely large M due to the linear scaling of both schemes, as expected from Lemma 4.

In Fig. 10, to investigate the massive-band case with large N , the net average harvested power is plotted against the total number of available sub-bands N for the case of SISO WET with $N_2 = 1$ and $M = 1$ (thus, phase-II training is no longer needed and the proposed two-phase training is the same as phase-I training only), where N varies from 20 to 2000 (by assuming that some other spectrum in addition to the 902-928MHz ISM band is available). The channel block length is set as $T = 50$ ms. It is observed that in the ideal case with perfect CSI at the ET, the average harvested power increases logarithmically with N , which is in accordance to Lemma 6. In contrast, for the proposed training scheme that takes into account the energy cost of channel training, the net harvested power saturates as N becomes large, as expected from Lemma 7. Furthermore, Fig. 10 shows that in this case, the asymptotic result given in (53) provides a satisfactory performance upper bound for the proposed training scheme with large N .

VII. CONCLUSIONS AND FUTURE WORK

This paper studies the energy-constrained training design for MISO WET systems in frequency-selective channels. By exploiting channel reciprocity, a two-phase training scheme is proposed. A closed-form expression is derived for the net harvested energy at the ER, based on which a training design optimization problem is formulated and optimally solved. Asymptotic analysis is also presented for systems with a large number of transmit antennas or independent frequency sub-bands to gain useful insights. Numerical results are provided to validate our analysis and

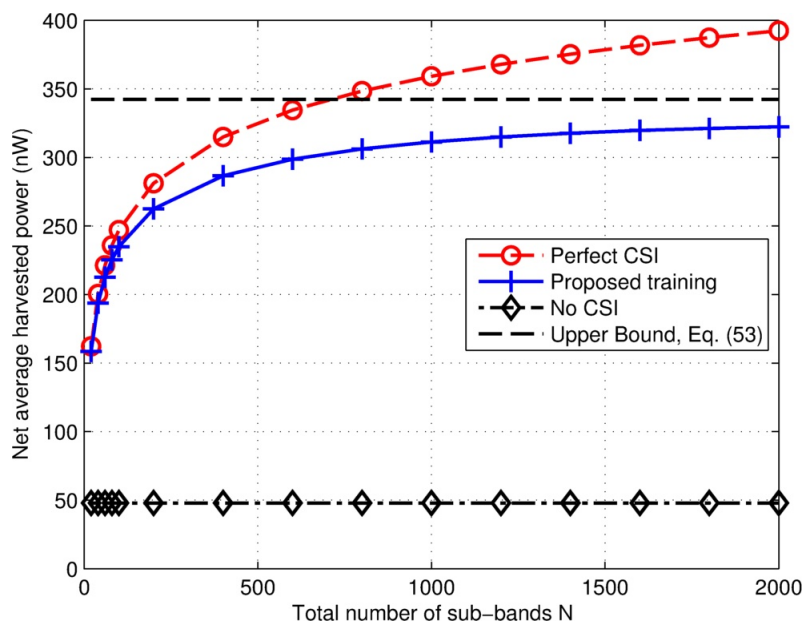


Fig. 10: Net average harvested power versus total number of sub-bands N for SISO WET.

demonstrate the effectiveness of the proposed scheme which optimally balances the achievable frequency-diversity and energy-beamforming gains in multi-antenna WET with limited-energy training.

There are a number of research directions along which the developed results in this paper can be further investigated, as briefly discussed in the following.

- *MIMO WET*: The optimal training design for the general MIMO wide-band WET systems remains an open problem. MIMO WET for flat-fading channels have been studied in [29]. However, the extension to the more complex frequency-selective channels is no-trivial and deserves further investigation.
- *Correlated Channel*: The analysis in this paper is based on the assumption of independent channels in both spatial and frequency domains, which practically holds with sufficient sub-band partition and antenna spacing. For the general setup with correlated channels, both the training optimization and performance analysis become more challenging; however, spatial and/or frequency channel correlations can also be exploited to reduce the training overhead and hence enhance the overall energy transfer efficiency.
- *Multi-User Setup*: More research endeavor is needed to find the optimal training design for the general multi-user setups with near-far located ERs. In this case, the so-called “double near-far” problem reported in [9], [29] needs to be addressed, where a far-away ER from the ET suffers from higher propagation loss than a close ER for both reverse-link channel training and forward-link energy transmission.
- *Energy Outage*: In this paper, the net average harvested power at the ER is maximized by optimizing the training design. In certain scenarios such as the delay-sensitive applications, a more appropriate design criterion may be minimizing the energy outage probability of ERs, for which the optimal training and energy transmission design still remain open.

APPENDIX A
ORDER STATISTIC

This appendix gives a brief introduction on order statistic, which is used for the proof of Lemma 1. A comprehensive treatment on this topic can be found in e.g. [30].

Definition 1: Let V_1, \dots, V_{N_1} be N_1 real-valued random variables. The order statistics $V_{[1]}, \dots, V_{[N_1]}$ are random variables defined by sorting the values of V_1, \dots, V_{N_1} in non-increasing order, i.e., $V_{[1]} \geq V_{[2]} \geq \dots \geq V_{[N_1]}$.

Lemma 8: Let V_1, \dots, V_{N_1} be N_1 i.i.d. real-valued random variables with cumulative distribution function (CDF) $F(v)$. The CDF of the n th order statistic $V_{[n]}$, denoted as $F_{[n]}(v)$, can be expressed as

$$F_{[n]}(v) = \sum_{k=0}^{n-1} \binom{N_1}{k} F(v)^{N_1-k} (1-F(v))^k, \quad n = 1, \dots, N_1. \quad (54)$$

APPENDIX B
A USEFUL LEMMA

Lemma 9: Let $\mathbf{v}_1, \dots, \mathbf{v}_{N_1} \in \mathbb{C}^{M \times 1}$ be N_1 i.i.d. zero-mean CSCG random vectors distributed as $\mathbf{v}_n \sim \mathcal{CN}(\mathbf{0}, \sigma_v^2 \mathbf{I}_M)$, $\forall n$. Further denote by $[\cdot]$ the permutation such that $\|\mathbf{v}_{[1]}\|^2 \geq \|\mathbf{v}_{[2]}\|^2 \geq \dots \geq \|\mathbf{v}_{[N_1]}\|^2$. Then we have

$$\mathbb{E} \left[\|\mathbf{v}_{[n]}\|^2 \right] = \sigma_v^2 G_n(N_1, M), \quad n = 1, \dots, N_1, \quad (55)$$

where $G_n(N_1, M)$, $n = 1, \dots, N_1$, is a function of N_1 and M given by

$$G_1(N_1, M) = \sum_{p=1}^{N_1} \binom{N_1}{p} (-1)^{p+1} c_p, \quad (56)$$

$$G_{n+1}(N_1, M) = G_n(N_1, M) - \Delta_n, \quad n = 1, \dots, N_1 - 1, \quad (57)$$

with

$$c_p = \sum_{k_0 + \dots + k_{M-1} = p} \binom{p}{k_0, \dots, k_{M-1}} \left(\prod_{m=0}^{M-1} \frac{1}{(m!)^{k_m}} \right) \left(\sum_{m=0}^{M-1} m k_m \right)! \frac{1}{p^{1 + \sum_{m=0}^{M-1} m k_m}}, \quad (58)$$

$$\Delta_n = \binom{N_1}{n} \sum_{l=0}^n \sum_{p=0}^{N_1-l} \binom{n}{l} \binom{N_1-l}{p} (-1)^{n-l+p} c_p. \quad (59)$$

Note that in (58), the summation is taken over all sequences of non-negative integer indices k_0 to k_{M-1} with the sum equal to p , and the coefficients $\binom{p}{k_0, \dots, k_{M-1}}$ are known as multinomial coefficients, which can be computed as

$$\binom{p}{k_0, \dots, k_{M-1}} = \frac{p!}{k_0! \dots k_{M-1}!}.$$

Furthermore, for $n = 1$ and $M = 1$, $G_n(N_1, M)$ can be expressed as the N_1 th partial sum of the harmonic series, i.e.,

$$G_1(N_1, 1) = \sum_{i=1}^{N_1} \frac{1}{i}. \quad (60)$$

Proof: Define the random variables $V_n \triangleq \|\mathbf{v}_n\|^2$, $n = 1, \dots, N_1$. It then follows that V_1, \dots, V_{N_1} are i.i.d. Erlang distributed with shape parameter M and rate $\lambda = 1/\sigma_v^2$, whose CDF is given by

$$F(v) = 1 - \sum_{m=0}^{M-1} \frac{1}{m!} e^{-\lambda v} (\lambda v)^m, \quad v \geq 0. \quad (61)$$

The CDF $F_{[n]}(v)$ of the order statistics $V_{[n]} \triangleq \|\mathbf{v}_{[n]}\|^2$ is then obtained by substituting $F(v)$ in (61) into (54). The expectations can then be expressed as

$$\mathbb{E}[V_{[n]}] = \int_0^\infty (1 - F_{[n]}(v)) dv, \quad n = 1, \dots, N_1. \quad (62)$$

We first show (55) for $n = 1$, i.e., the expectation of the maximum of N_1 i.i.d. Erlang random variables. By substituting $n = 1$ into (54), we have $F_{[1]}(v) = F(v)^{N_1}$. With binomial expansion, we then have

$$\begin{aligned} \mathbb{E}[V_{[1]}] &= \int_0^\infty \left(1 - \left(1 - \sum_{m=0}^{M-1} \frac{1}{m!} e^{-\lambda v} (\lambda v)^m \right)^{N_1} \right) dv \\ &= \sum_{p=1}^{N_1} \binom{N_1}{p} (-1)^{p+1} a_p, \end{aligned} \quad (63)$$

where

$$\begin{aligned} a_p &= \int_0^\infty e^{-\lambda p v} \left(\sum_{m=0}^{M-1} \frac{1}{m!} (\lambda v)^m \right)^p dv \\ &= \sum_{k_0 + \dots + k_{M-1} = p} \binom{p}{k_0, \dots, k_{M-1}} \left(\prod_{m=0}^{M-1} \frac{1}{(m!)^{k_m}} \right) \lambda^{\sum_{m=0}^{M-1} m k_m} \int_0^\infty e^{-\lambda p v} v^{\sum_{m=0}^{M-1} m k_m} dv \\ &= \frac{1}{\lambda} c_p = \sigma_v^2 c_p, \end{aligned} \quad (64)$$

$$= \frac{1}{\lambda} c_p = \sigma_v^2 c_p, \quad (65)$$

where (64) follows from the multinomial expansion theorem, and (65) follows from the integral identity $\int_0^\infty x^n e^{-\mu x} dx = n! \mu^{-n-1}$ [33]. The result in (55) for $n = 1$ then follows by substituting (65) into (63).

To show (55) for $n \geq 2$, we apply the following recursive relationship obtained from (54):

$$F_{[n+1]}(v) = F_{[n]}(v) + \binom{N_1}{n} F(v)^{N_1-n} (1 - F(v))^n, \quad n = 1, \dots, N_1 - 1. \quad (66)$$

By substituting (66) into (62), we get

$$\mathbb{E}[V_{[n+1]}] = \mathbb{E}[V_{[n]}] - \int_0^\infty \binom{N_1}{n} F(v)^{N_1-n} (1 - F(v))^n dv. \quad (67)$$

By evaluating the integration in (67), the result in (55) for $n \geq 2$ can be obtained.

Furthermore, by substituting $M = 1$ into (56) and with some manipulations, the expression for $G_1(N_1, 1)$ as given in (60) can be obtained. The property of $G_n(N_1, M)$ given in (15) can be verified as well.

This completes the proof of Lemma 9. ■

APPENDIX C

PROOF OF LEMMA 1

Note that in the absence of phase-I training ($E_1 = 0$), the distribution of $\mathbf{h}_{[n]}$ simply follows from (1), which thus leads to $\mathbb{E} \left[\|\mathbf{h}_{[n]}\|^2 \right] = \beta M, \forall n$. In this case, no frequency-diversity gain is achieved. For the general scenario with $E_1 > 0$, $[n]$ is the n th strongest sub-band out of the N_1 trained sub-bands as determined via (12). As a consequence, the statistics of the channel $\mathbf{h}_{[n]}$ are affected by phase-I training via (11) and (12). To exploit such a relationship, we first show the following lemma.

Lemma 10: The input-output relationship in (11) is statistically equivalent to

$$\mathbf{h}_n = \frac{\beta\sqrt{E_1}}{\beta E_1 + N_0} \mathbf{y}_n^I + \sqrt{\frac{\beta N_0}{\beta E_1 + N_0}} \mathbf{t}_n, \quad n \in \mathcal{N}_1, \quad (68)$$

where $\mathbf{t}_n \sim \mathcal{CN}(\mathbf{0}, \mathbf{I}_M)$ is a CSCG random vector independent of \mathbf{y}_n^I , i.e., $\mathbb{E} [\mathbf{y}_n^I \mathbf{t}_n^H] = \mathbf{0}, n \in \mathcal{N}_1$.

Proof: It follows from (1) and (11) that \mathbf{y}_n^I is a CSCG random vector distributed as

$$\mathbf{y}_n^I \sim \mathcal{CN}(\mathbf{0}, (\beta E_1 + N_0) \mathbf{I}_M), \quad \forall n. \quad (69)$$

Furthermore, the cross-correlation between \mathbf{h}_n and \mathbf{y}_n^I is

$$\mathbb{E} [\mathbf{y}_n^I \mathbf{h}_n^H] = \beta \sqrt{E_1} \mathbf{I}_M. \quad (70)$$

Since both \mathbf{h}_n and \mathbf{y}_n are zero-mean CSCG random vectors, to prove Lemma 10, it is sufficient to show that the random vector \mathbf{h}_n obtained by (68) has the same distribution as (1), and also has the same cross-correlation with \mathbf{y}_n^I as (70). Such results can be easily verified from (68) and (69). \blacksquare

By applying Lemma 10 for the N_2 selected sub-bands as determined in (12), we obtain the following result,

$$\mathbb{E} \left[\|\mathbf{h}_{[n]}\|^2 \right] = \frac{\beta^2 E_1}{(\beta E_1 + N_0)^2} \mathbb{E} \left[\|\mathbf{y}_{[n]}^I\|^2 \right] + \frac{\beta N_0 M}{\beta E_1 + N_0} \quad (71)$$

$$= \frac{\beta^2 E_1 G_n(N_1, M) + \beta N_0 M}{\beta E_1 + N_0}, \quad n = 1, \dots, N_2, \quad (72)$$

where (72) follows from Lemma 9 in Appendix B and (69).

This completes the proof of Lemma 1.

APPENDIX D

PROOF OF LEMMA 2

Since both $\mathbf{h}_{[n]}$ and $\mathbf{y}_{[n]}^{\text{II}}$ are zero-mean random vectors with i.i.d. entries, the LMMSE estimator can be expressed as $\hat{\mathbf{h}}_{[n]} = b_n \mathbf{y}_{[n]}^{\text{II}}$, with b_n a complex-valued parameter to be determined. The corresponding MSE can be expressed as

$$\begin{aligned} e_n &= \mathbb{E} \left[\|\tilde{\mathbf{h}}_{[n]}\|^2 \right] = \mathbb{E} \left[\left\| \left(1 - b_n \sqrt{E_{2,n}} \right) \mathbf{h}_{[n]} - b_n \mathbf{z}_{[n]}^{\text{II}} \right\|^2 \right] \\ &= \left| 1 - b_n \sqrt{E_{2,n}} \right|^2 R_n(N_1, E_1) + |b_n|^2 N_0 M \\ &= |b_n|^2 (E_{2,n} R_n(N_1, E_1) + N_0 M) - (b_n + b_n^*) \sqrt{E_{2,n}} R_n(N_1, E_1) + R_n(N_1, E_1). \end{aligned}$$

By setting the derivative of e_n with respect to b_n^* equal to zero, the optimal coefficient b_n can be obtained as

$$b_n = \frac{\sqrt{E_{2,n}R_n(N_1, E_1)}}{E_{2,n}R_n(N_1, E_1) + N_0M}, \quad n = 1, \dots, N_2.$$

The resulting MMSE can be obtained accordingly. Furthermore, the following result can be obtained,

$$\mathbb{E} \left[\|\hat{\mathbf{h}}_{[n]}\|^2 \right] = |b_n|^2 \mathbb{E} \left[\|\mathbf{y}_{[n]}^{\text{II}}\|^2 \right] = \frac{E_{2,n}R_n^2(N_1, E_1)}{E_{2,n}R_n(N_1, E_1) + N_0M}, \quad n = 1, \dots, N_2. \quad (73)$$

To show that $\mathbb{E} \left[\tilde{\mathbf{h}}_{[n]}^H \hat{\mathbf{h}}_{[n]} \right] = 0$, we use the following result,

$$\mathbb{E} \left[\mathbf{h}_{[n]}^H \hat{\mathbf{h}}_{[n]} \right] = b \mathbb{E} \left[\mathbf{h}_{[n]}^H \mathbf{y}_{[n]}^{\text{II}} \right] = \frac{E_2 R_h^2(N_1, E_1)}{E_2 R_h(N_1, E_1) + N_0M} = \mathbb{E} \left[\|\hat{\mathbf{h}}_{[n]}\|^2 \right]. \quad (74)$$

Therefore, we have

$$\mathbb{E} \left[\tilde{\mathbf{h}}_{[n]}^H \hat{\mathbf{h}}_{[n]} \right] = \mathbb{E} \left[\mathbf{h}_{[n]}^H \hat{\mathbf{h}}_{[n]} \right] - \mathbb{E} \left[\|\hat{\mathbf{h}}_{[n]}\|^2 \right] = 0, \quad n = 1, \dots, N_2, \quad (75)$$

where we have used the identity $\tilde{\mathbf{h}}_{[n]} = \mathbf{h}_{[n]} - \hat{\mathbf{h}}_{[n]}$.

This completes the proof of Lemma 2.

APPENDIX E

PROOF OF LEMMA 4

By applying (46) to (14), we have $R_n^{\text{large-}M}(N_1, E_1) \rightarrow \beta M, \forall n = 1, \dots, N_2$. As a result, the average harvested energy at the ER in (21) reduces to

$$\bar{Q}^{\text{large-}M}(\{E_{2,n}\}) \rightarrow \eta T P_s \beta \sum_{n=1}^{N_2} \frac{\beta M E_{2,n} + N_0}{\beta E_{2,n} + N_0}, \quad (76)$$

which is independent of E_1 and N_1 . Therefore, we should have $E_1^{\text{large-}M} \rightarrow 0$, i.e., the phase-I training for exploiting the frequency-diversity gain is no longer required. In this case, N_2 out of the N total available sub-bands can be arbitrarily selected for phase-II training in order to apply energy beamforming. Based on (24), the optimal training energy for each of the N_2 sub-bands reduces to

$$\begin{aligned} E_{2,n}^{\text{large-}M} &\rightarrow \left[\sqrt{\eta T P_s (M-1) N_0} - \frac{N_0}{\beta} \right]^+ \\ &\rightarrow \sqrt{\eta T P_s N_0 M}, \quad n = 1, \dots, N_2, \quad \text{as } M \rightarrow \infty. \end{aligned}$$

Furthermore, based on (36), the corresponding net harvested energy reduces to

$$\begin{aligned} \bar{Q}_{\text{net}}^{\text{large-}M} &\rightarrow N_2 \left(\eta T P_s \beta M - 2 \sqrt{\eta T P_s N_0 (M-1)} + \frac{N_0}{\beta} \right) \\ &\rightarrow \eta T N_2 P_s \beta M, \quad \text{as } M \rightarrow \infty. \end{aligned}$$

This completes the proof of Lemma 4.

APPENDIX F
PROOF OF LEMMA 6

To prove Lemma 6, we first show the following result.

Lemma 11: For the function $G_n(N_1, M)$ defined in Lemma 9 in Appendix B, the following inequality holds:

$$G_n(N_1, M) \leq MG_1(N_1, 1), \forall n = 1, \dots, N_2. \quad (77)$$

Proof: Since $G_n(N_1, M)$ monotonically decreases with n as given in (15), to prove Lemma 11, it is sufficient to show that $G_1(N_1, M) \leq MG_1(N_1, 1)$. To this end, we define N_1 i.i.d. zero-mean CSCG random vectors $\mathbf{u}_i \sim \mathcal{CN}(\mathbf{0}, \mathbf{I}_M)$, $i = 1, \dots, N_1$. Then based on the definition of $G_n(N_1, M)$ given in (55), we have

$$\begin{aligned} G_1(N_1, M) &= \mathbb{E} \left[\max_{i=1, \dots, N_1} \|\mathbf{u}_i\|^2 \right] = \mathbb{E} \left[\max_{i=1, \dots, N_1} \sum_{j=1}^M |u_{ij}|^2 \right] \\ &\leq \mathbb{E} \left[\sum_{j=1}^M \max_{i=1, \dots, N_1} |u_{ij}|^2 \right] = \sum_{j=1}^M \mathbb{E} \left[\max_{i=1, \dots, N_1} |u_{ij}|^2 \right] \\ &= MG_1(N_1, 1), \end{aligned}$$

where $u_{ij} \sim \mathcal{CN}(0, 1)$ denotes the j th element of \mathbf{u}_i . Note that the last equality follows from the definition of $G_1(N, 1)$ and the fact that for any fixed j , $\{u_{ij}\}_{i=1}^{N_1}$ are i.i.d. zero-mean unit-variance CSCG random variables. ■

With the expression in (51), the average harvested energy with perfect CSI at the ET is upper-bounded as

$$\bar{Q}^{\text{ideal}}(N) = \eta TP_s \beta \sum_{n=1}^{N_2} G_n(N, M) \leq \eta TP_s \beta N_2 MG_1(N, 1), \quad (78)$$

where the inequality follows from Lemma 11. Furthermore, it is easy to see that $\bar{Q}^{\text{ideal}}(N)$ is lower-bounded as

$$\bar{Q}^{\text{ideal}}(N) = \eta TP_s \beta \sum_{n=1}^{N_2} G_n(N, M) \geq \eta TP_s \beta G_1(N, M) \geq \eta TP_s \beta G_1(N, 1), \quad (79)$$

where the last inequality follows since $G_1(N, M)$ monotonically increases with M . It follows from (78) and (79) that $\bar{Q}^{\text{ideal}}(N)$ should have the same asymptotic scaling with N as $G_1(N, 1)$. Furthermore, for sufficiently large N , it follows from (60) that $G_1(N, 1)$ can be expressed as

$$G_1(N, 1) = \sum_{i=1}^N \frac{1}{i} = \ln N + \gamma + \epsilon_N, \quad (80)$$

where $\gamma \approx 0.5772$ is the Euler-Mascheroni constant and $\epsilon \sim \frac{1}{2N}$ which approaches 0 as N increases. Therefore, for $N \rightarrow \infty$, the following inequalities hold,

$$\eta TP_s \beta \ln N \leq \bar{Q}^{\text{ideal}}(N) \leq \eta TP_s \beta N_2 M \ln N, \quad (81)$$

or $\bar{Q}^{\text{ideal}}(N) = \Theta(\ln N)$. This thus completes the proof of Lemma 6.

APPENDIX G
PROOF OF LEMMA 7

To prove Lemma 7, we first derive an upper bound for the net harvested energy $\bar{Q}_{\text{net}}(N_1, E_1, \{E_{2n}\})$ of the two-phase training scheme for arbitrary N_1 , E_1 , and $\{E_{2,n}\}$. Based on (22), we have

$$\begin{aligned}\bar{Q}_{\text{net}}(N_1, E_1, \{E_{2n}\}) &\leq \eta T P_s \sum_{n=1}^{N_2} R_n(N_1, E_1) - E_1 N_1 \\ &= \eta T P_s \beta \sum_{n=1}^{N_2} \frac{\beta E_1 G_n(N_1, M) + N_0 M}{\beta E_1 + N_0} - E_1 N_1 \\ &\leq \eta T P_s \beta N_2 M \frac{\beta E_1 G_1(N_1, 1) + N_0}{\beta E_1 + N_0} - E_1 N_1 \\ &\triangleq \bar{Q}_{\text{net}}^{\text{UB}}(N_1, E_1),\end{aligned}$$

where the last inequality follows from Lemma 11 in Appendix F. Note that the above bound is tight for $M = 1$ and $N_2 = 1$. As a result, the net harvested energy achieved by the optimized training scheme is upper-bounded by the optimal value of the following problem.

$$\begin{aligned}\text{(P1-UB):} \quad &\max_{N_1, E_1} \bar{Q}_{\text{net}}^{\text{UB}}(N_1, E_1) \triangleq \eta T P_s \beta N_2 M \frac{\beta E_1 G_1(N_1, 1) + N_0}{\beta E_1 + N_0} - E_1 N_1 \\ &\text{subject to } N_2 \leq N_1 \leq N, \\ &E_1 \geq 0.\end{aligned}$$

With N_1 fixed, (P1-UB) is a convex optimization problem with respect to E_1 , whose optimal solution can be expressed as

$$E_1^{\text{UB}\star}(N_1) = \left[\sqrt{\frac{\eta T P_s N_2 M N_0 (G_1(N_1, 1) - 1)}{N_1}} - \frac{N_0}{\beta} \right]^+ . \quad (82)$$

The corresponding optimal value of (P1-UB) as a function of N_1 can be expressed as

$$\bar{Q}_{\text{net}}^{\text{UB}}(N_1) = \begin{cases} \eta T P_s N_2 M \beta, & \text{if } G_1(N_1, 1) - 1 < \frac{N_1}{\Gamma N_2 M} \\ \eta T P_s N_2 M \beta \left(1 + \left(\sqrt{G_1(N_1, 1) - 1} - \sqrt{\frac{N_1}{\Gamma N_2 M}} \right)^2 \right), & \text{otherwise.} \end{cases} \quad (83)$$

Therefore, problem (P1-UB) reduces to finding the optimal number of training sub-bands as

$$\max_{N_2 \leq N_1 \leq N} \bar{Q}_{\text{net}}^{\text{UB}}(N_1). \quad (84)$$

It follows from (83) that if Γ is small such that $G_1(N_1, 1) - 1 < \frac{N_1}{\Gamma N_2 M}$, $\forall N_1$, $\bar{Q}_{\text{net}}^{\text{UB}}$ is independent of N_1 and hence problem (84) has the trivial optimal value $\eta T P_s N_2 M \beta$, which is smaller than the right hand side (RHS) of (53).

On the other hand, for the non-trivial scenario with moderately large Γ values, problem (84) reduces to

$$\max_{N_2 \leq N_1 \leq N} \sqrt{G_1(N_1, 1) - 1} - \sqrt{\frac{N_1}{\Gamma N_2 M}}. \quad (85)$$

Problem (85) is a discrete optimization problem due to the integer constraint on N_1 . To obtain an approximate closed-form solution to (85), we first apply the following approximation for the harmonic sum,

$$G_1(N_1, 1) = \sum_{i=1}^{N_1} \frac{1}{i} = \ln N_1 + \gamma + \epsilon_{N_1} \approx \ln N_1 + 1.$$

Furthermore, by relaxing the integer constraint and with asymptotically large N and moderate N_2 values, problem (85) can be approximated as

$$\max_{\bar{N}_1} \sqrt{\ln \bar{N}_1} - \sqrt{\frac{\bar{N}_1}{\Gamma N_2 M}}. \quad (86)$$

By setting the derivative to zero, the optimal solution \bar{N}_1^* to problem (86) satisfies

$$\bar{N}_1^* \ln \bar{N}_1^* = \Gamma N_2 M, \text{ or } \ln \bar{N}_1^* e^{\ln \bar{N}_1^*} = \Gamma N_2 M. \quad (87)$$

Based on the definition of the Lambert W function, \bar{N}_1^* in (87) can be expressed as $\bar{N}_1^* = e^{W(\Gamma N_2 M)}$, and the corresponding optimal value of problem (84) can be obtained as

$$\bar{Q}_{\text{net}}^{\text{UB}*} \approx \eta T N_2 P_2 \beta M \left(1 + \left(\sqrt{W(\Gamma N_2 M)} - \frac{1}{\sqrt{W(\Gamma N_2 M)}} \right)^2 \right). \quad (88)$$

This thus completes the proof of Lemma 7.

REFERENCES

- [1] H. J. Visser and R. J. M. Vullers, "RF energy harvesting and transport for wireless sensor network applications: Principles and requirements," *Proceedings of the IEEE*, vol. 101, no. 6, pp. 1410–1423, Jun. 2013.
- [2] S. Bi, C. K. Ho, and R. Zhang, "Wireless powered communication: opportunities and challenges," to appear in *IEEE Commun. Mag.*, available online at <http://arxiv.org/abs/1408.2335>.
- [3] X. Lu, P. Wang, D. Niyato, D. I. Kim, and Z. Han, "Wireless networks with RF energy harvesting: a contemporary survey," to appear in *IEEE Commun. Surveys Tuts.*, available online at <http://arxiv.org/abs/1406.6470>.
- [4] W. C. Brown, "The history of power transmission by radio waves," *IEEE Trans. on Microwave Theory and Techniques*, vol. MTT-32, no. 9, pp. 1230–1242, Sep. 1984.
- [5] J. O. Mcspadden and J. C. Mankins, "Space solar power programs and microwave wireless power transmission technology," *IEEE Microw. Mag.*, vol. 3, no. 4, pp. 46–57, Dec. 2002.
- [6] R. Zhang and C. K. Ho, "MIMO broadcasting for simultaneous wireless information and power transfer," *IEEE Trans. Wireless Commun.*, vol. 12, no. 5, pp. 1989–2001, May 2013.
- [7] X. Zhou, R. Zhang, and C. K. Ho, "Wireless information and power transfer: architecture design and rate-energy tradeoff," *IEEE Trans. Commun.*, vol. 61, no. 11, pp. 4757–4767, Nov. 2013.
- [8] L. Liu, R. Zhang, and K. C. Chua, "Wireless information transfer with opportunistic energy harvesting," *IEEE Trans. Wireless Commun.*, vol. 12, no. 1, pp. 288–300, Jan. 2013.
- [9] H. Ju and R. Zhang, "Throughput maximization in wireless powered communication networks," *IEEE Trans. Wireless Commun.*, vol. 13, no. 1, pp. 418–428, Jan. 2014.
- [10] S. Lee, R. Zhang, and K. Huang, "Opportunistic wireless energy harvesting in cognitive radio networks," *IEEE Trans. Wireless Commun.*, vol. 12, no. 9, pp. 4788–4799, Sep. 2013.
- [11] X. Lu, P. Wang, D. Niyato, and E. Hossain, "Dynamic spectrum access in cognitive radio networks with RF energy harvesting," *IEEE Wireless Commun.*, pp. 102–110, Jun. 2014.

- [12] A. A. Nasir, X. Zhou, S. Durrani, and R. A. Kennedy, "Relaying protocols for wireless energy harvesting and information processing," *IEEE Trans. Wireless Commun.*, vol. 12, no. 7, pp. 3622–3636, Jul. 2013.
- [13] Z. Ding, S. M. Perlaza, I. Esnaola, and H. V. Poor, "Power allocation strategies in energy harvesting wireless cooperative networks," *IEEE Trans. Wireless Commun.*, vol. 13, no. 2, pp. 846–860, Feb. 2014.
- [14] Y. Zeng and R. Zhang, "Full-duplex wireless-powered relay with self-energy recycling," submitted to *IEEE Wireless Commun. Lett.*, available online at <http://arxiv.org/abs/1411.3061>.
- [15] H. Ju and R. Zhang, "User cooperation in wireless powered communication networks," to appear in *IEEE Global Communications Conference (GLOBECOM)*, 2014, available online at <http://arxiv.org/abs/1403.7123>.
- [16] F. Rusek, D. Persson, B. K. Lau, E. G. Larsson, T. L. Marzetta, O. Edfors, and F. Tufvesson, "Scaling up MIMO: Opportunities and challenges with very large arrays," *IEEE Signal Process. Mag.*, vol. 30, no. 1, pp. 40–60, Jan. 2013.
- [17] L. Lu, G. Y. Li, A. L. Swindlehurst, A. Ashikhin, and R. Zhang, "An overview of massive MIMO: benefits and challenges," *IEEE J. Sel. Topics Signal Process.*, vol. 8, no. 5, pp. 742–758, Oct. 2014.
- [18] G. Yang, C. K. Ho, R. Zhang, and Y. L. Guan, "Throughput optimization for massive MIMO systems powered by wireless energy transfer," to appear in *IEEE J. Sel. Areas Commun.*, available online at <http://arxiv.org/abs/1403.3991>.
- [19] P. Grover and A. Sahai, "Shannon meets tesla: Wireless information and power transfer," in *Int. Symp. on Inf. Theory*, Jun. 2010, pp. 2363–2367.
- [20] FCC Rules and Regulations Part 15 Section 247, Operation within the bands 902-928 MHz, 2400-2483.5 MHz, and 5725-5850 MHz.
- [21] D. W. K. Ng, E. S. Lo, and R. Schober, "Wireless information and power transfer: Energy efficiency optimization in OFDMA systems," *IEEE Trans. Wireless Commun.*, vol. 12, no. 12, pp. 6352–6370, Dec. 2013.
- [22] X. Zhou, R. Zhang, and C. K. Ho, "Wireless information and power transfer in multiuser OFDM systems," *IEEE Trans. Wireless Commun.*, vol. 13, no. 4, pp. 2282–2294, Apr. 2014.
- [23] K. Huang and E. Larsson, "Simultaneous information and power transfer for broadband wireless systems," *IEEE Trans. Signal Process.*, vol. 61, no. 23, pp. 5972–5986, Dec. 2013.
- [24] G. Yang, C. K. Ho, and Y. L. Guan, "Dynamic resource allocation for multiple-antenna wireless power transfer," *IEEE Trans. Signal Process.*, vol. 62, no. 14, pp. 3565 – 3577, Jun. 2014.
- [25] X. Chen, C. Yuen, and Z. Zhang, "Wireless energy and information transfer tradeoff for limited-feedback multiantenna systems with energy beamforming," *IEEE Trans. Veh. Technol.*, vol. 63, no. 1, pp. 407–412, Jan. 2014.
- [26] D. J. Love, R. W. Heath Jr., V. K. N. Lau, D. Gesbert, B. D. Rao, and M. Andrews, "An overview of limited feedback in wireless communication systems," *IEEE J. Sel. Areas Commun.*, vol. 26, no. 8, pp. 1341–1365, Oct. 2008.
- [27] T. L. Marzetta, "Noncooperative cellular wireless with unlimited numbers of base station antennas," *IEEE Trans. Wireless Commun.*, vol. 9, no. 11, pp. 3590–3600, Nov. 2010.
- [28] J. Xu and R. Zhang, "Energy beamforming with one-bit feedback," *IEEE Trans. Signal Process.*, vol. 62, no. 20, pp. 5370–5381, Oct. 2014.
- [29] Y. Zeng and R. Zhang, "Optimized training design for wireless energy transfer," to appear in *IEEE Trans. Commun.*, available online at <http://arxiv.org/abs/1403.7870>.
- [30] H. A. David and H. N. Nagaraja, *Order Statistics*, 3rd ed. John Wiley & Sons, Inc., Hoboken, New Jersey, 2003.
- [31] D. Tse and P. Viswanath, *Fundamentals of Wireless Communication*. Cambridge University Press, 2005.
- [32] T. S. Rappaport, *Wireless Communications: Principles and Practice*. Prentice Hall, 2002.
- [33] I. Gradshteyn and I. M. Ryzhik, *Table of integrals, series and products*, 7th ed. Elsevier Academic Press, 2007.